VI. THE MINERALOGY OF THE LAYERED SEQUENCE

A. ORTHOPYROXENE

1. Introduction

An interest in the orthopyroxene-pigeonite relationships was stimulated by a study of rocks from the Main Zone of the Bushveld Complex in the Kruis River area (Von Gruenewaldt, 1966). Consequently, prior to the mapping of the area under consideration in this treatise, detailed investigations of the Ca-poor pyroxenes were started on specimens from different localities, especially from Dsjate 249 KT in Sekhukhuneland and from Bon Accord north of Pretoria. These earlier investigations have been supplemented by the results of the study of specimens from the Tauteshoogte-Roossenekal area. This has made it possible to reconstruct the sequence of events leading to the crystallization of pigeonite from the Bushveld magma. Portions of the results were published recently (Von Gruenewaldt, 1970).

2. Determinative methods

The composition of the orthopyroxene was determined from 2V measurements and by refractive index determinations of n_z. $2V_x$ measurements were made on grain-mounts of separated orthopyroxene and the values given in Appendix I represent the average values of between 8 and 10 direct readings of both optical axes under conoscopic illumination. The measurements were corrected for the set of hemispheres used with the aid of the diagrams constructed from the nomogram by Tröger (1959, p. 124) and the composition was evaluated by using the graph of Hess (Tröger, 1959, p. 59). Judging from the scatter of points on this graph (Deer et al., 1963, Fig. 10, p. 28) the accuracy of this method is probably greater than $\pm$ 5 mole per cent. In the compositional range Fs_{45-55} use was made of refractive index determinations by the immersion method. The liquids used were mixtures of monobromonaphthalene and methylene iodide, and the index of refraction of these mixtures was determined with a Leitz-Jelley refractometer. The accuracy of this method is considered to be $\pm$ 0,002 which corresponds to $\pm$ 3 mole per cent.

Five samples of separated orthopyroxene from Dsjate 249 KT were submitted for chemical analyses to the National Institute for Metallurgy. Separation to a purity of above 98,5 per cent was achieved with the Franz Isodynamic Separator, the only impurity being augite. The analyses given in Table III were

corrected for impurities by determining optically the composition of the co-existing augite. The analyses differ therefore slightly from those published recently (Von Gruenewaldt, 1970, p. 68) although the published Fe:Mg:Ca ratios are based on the corrected analyses. From the corrected analyses the structural formulae (Table III) were calculated using the method outlined by Hess (1949, p. 625).

3. Compositional Variations (Folder III)

No samples of the Merensky Reef were available from bore-hole PB1, but Roux (1968, p. 70) found that the orthopyroxene of this reef, directly east of the mapped area, has a composition of approximately Fs_{20}. The orthopyroxene in samples from the first 90m above the reef varies in composition between Fs_{20} and Fs_{25}. At 93m the composition rises abruptly to Fs_{34} and from the abundance of thick exsolution-lamellae of augite in the orthopyroxene, it is concluded that this is the first inverted pigeonite in the sequence. The presence of inverted pigeonite at this level in the intrusion is highly anomalous and no explanation for its presence can be offered at this stage. Plagioclase also changes in composition from An_{76} to An_{68} in these rocks. This zone is only a few metres thick and at its top the Fe-content of the orthopyroxene decreases gradually to Fs_{25}, 150m above the Merensky Reef. A similar break in the compositional trend was observed by Molyneux (1970, Fig. 12) about 300m above this reef on the Dsjate traverse.

From here onwards the composition of the orthopyroxene changes very gradually, apart from a small break about 1150m above the Merensky Reef (Folder III), to Fs_{44} below the fine-grained norite which underlies the Pyroxenite Marker of the Main Zone. The orthopyroxene of this fine-grained norite, although considerably enriched in the En molecule (Fs_{32-33}) is still inverted pigeonite but at the base of the Pyroxenite Marker the magma moved back into the field of crystallization of primary orthopyroxene with composition of Fs_{27}. These low Fs values are maintained upwards in the succession for about 300m from where the composition changes fairly rapidly to Fs_{44} below the Main Magnetitite Seam.

For the greater part of Subzones B and C of the Upper Zone, the composition of the orthopyroxene fluctuates between Fs_{40} and Fs_{46} and the iron content only increases to Fs_{50} in the topmost 100m of Subzone C. According to Molyneux (1970, p. 41) the erratic variation in composition of the orthopyroxene

in these two subzones may possibly be ascribed to the periodic extraction of iron from the magma during crystallization of the magnetitite seams. The pyroxenite of the Upper Zone (G649) in this area was found to contain inverted pigeonite (Fs_{43}) in contrast to the correlated horizon at Magnet Heights where it contains primary orthopyroxene (Molyneux, 1970, p. 41). The rocks of Subzone D only contain orthopyroxene for short distances above and below Seam 21. The composition of this orthopyroxene is Fs_{53} below the seam and changes rapidly to Fs_{62} (G368) about 40m above the seam. Molyneux (1970, p. 41) found orthopyroxene, 210m above Seam 21, to have a composition of Fs_{71}, which corresponds to the most Fe-rich intercumulus orthopyroxene in this area (Atkins, 1969, p. 241, ferrodiorite from Duikerkrans, S. A. 1143). Samples collected at higher levels than G368 and used in this investigation, did not contain any orthopyroxene.

4. Textural Features

a) General description of the textural variations

For the greater part of Subzone A of the Main Zone, the orthopyroxene is present as cumulus crystals, varying in size from about 1,6 x 0,7mm in the normal gabbroic rocks to 4,7 x 3,0mm in the so-called "porphyritic norites". The larger orthopyroxene grains usually contain small laths of plagioclase (Fig. 33) which would indicate that the latter was the first mineral to crystallize, and that the orthopyroxene had a higher growth rate. The size of the enclosed plagioclase laths may vary considerably, apparently depending on the time lapse between the onset of crystallization of the plagioclase and the onset of crystallization of the orthopyroxene.

There is an important textural change 1000m above the Merensky Reef, where the orthopyroxene changes from cumulus to intercumulus. The term "ophitic" would be more fitting for this texture because the orthopyroxene (Fs_{32}) forms units optically continuous over large areas which may completely enclose numerous plagioclase crystals (Fig. 34). In the field these units are readily recognizable because the parallel cleavage planes reflect the sunlight over areas up to 30cm in diameter on large boulders (Fig. 35). One hundred and fifty metres above the first appearance of ophitic orthopyroxene there is a compositional break (Folder III) and for 50m upwards typical cumulus orthopyroxene (Fs_{27}) is again encountered. Where the composition changes back to Fs_{32}, about 1200m above the Merensky Reef, the orthopyroxene is again "ophitic".

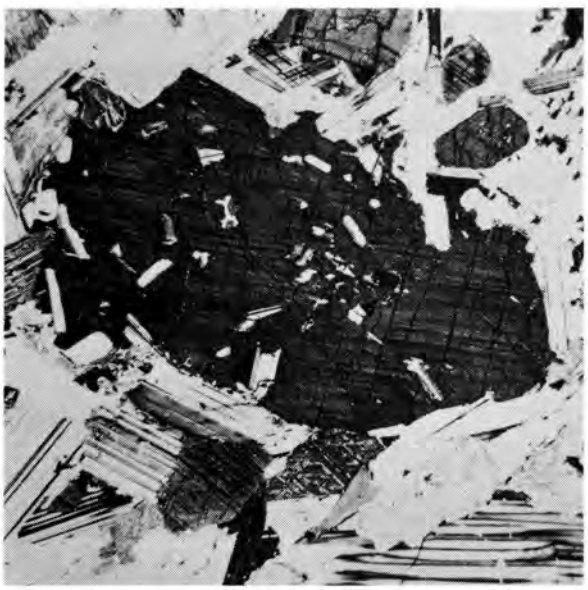

Fig. 33. Large orthopyroxene crystal which contains small inclusions of plagioclase. PB 3051. Crossed nicols, x12.

Fig. 34. Primary ophitic orthopyroxene. Specimen PB 717. Crossed nicols, x20.

Fig. 35. A large unit of similarly orientated orthopyroxene crystals which reflect the sunlight. Chieftains Plain 46 JT.

Almost simultaneously with this textural change of the hypersthene, the first inverted pigeonite appears in the sequence. This is characterized by the presence of numerous exsolution-lamellae of augite, which are considerably thicker than the fine striae common in primary orthopyroxene. The term "inverted pigeonite" is generally used for orthopyroxene which has originated from pigeonite owing to inversion of the latter (Brown, 1967, p. 349). This inverted pigeonite is present as small, irregularly shaped grains, usually enclosed in or surrounded by augite. It is very seldom found close to the primary ophitic orthopyroxene in thin sections. Two Ca-poor pyroxenes coexist for 1125mof the sequence in this area, i.e. up to the level in the intrusion where inverted pigeonite is the only Ca-poor pyroxene present. The change in composition of the orthopyroxene over this height is from Fs_{32} to about Fs_{37}.

Of interest is the observation that the level in the intrusion where inverted pigeonite becomes the only Ca-poor pyroxene, seems to rise from north to south. On the Dsjate traverse this level is taken at 1400m above the Merensky Reef (Molyneux, 1970, p. 33; Von Gruenewaldt, 1970, p. 69). On Mooimeisjesfontein, 50km south of Dsjate, Molyneux (1970, p. 33) records the appearance of inverted pigeonite 1900m above the Merensky Reef, whereas in this area, 40km south of Mooimeisjesfontein inverted pigeonite proper appears at 2325m above the Merensky Reef. In all three localities, the composition of this inverted pigeonite is about Fs_{36-37}. On Dsjate 249 KT, however, the first small grains of inverted pigeonite appeared at 1100m above the Merensky Reef with a composition of Fs_{33} for the primary hypersthene (Von Gruenewaldt, 1970, p. 69). This corresponds very closely to the appearance of inverted pigeonite in this area.

Inverted pigeonite is the only Ca-poor pyroxene up to the level of the Pyroxenite Marker, where primary cumulus orthopyroxene takes its place. From the Pyroxenite Marker up to the base of the Upper Zone there is a repetition of the observed textural features in the lower 3250m of the Main Zone. Cumulus orthopyroxene is present for 450m above the marker, where it is replaced by the ophitic variety. Simultaneously, small grains of inverted pigeonite, associated with clinopyroxene, make their appearance. Over the next 190m these two phases coexist, and from 50m below the Upper Zone inverted pigeonite (Fs_{37}) is the only Ca-poor pyroxene present in the remainder of the intrusion.

Characteristic of all the rocks in the sequence where cumulus inverted

pigeonite is developed, is the fact that they are present as groups of grains which possess similar orientations. This feature, together with the observed exsolution textures is discussed in detail in the following section.

In the rocks of the "orthopyroxene-pigeonite transition" (Folder III) there is a gradual change in the character of the ophitic hypersthene upwards in the succession. As mentioned already, at the base of this "transition zone", the orthopyroxene is typically ophitic. In this hypersthene the plagioclase has well developed crystal faces (Fig. 34), but at succeedingly higher levels the boundaries between the plagioclase and the ophitic orthopyroxene become more and more irregular. Gradually the ophitic hypersthene takes on the shape of separate cumulus crystals, although still optically continuous over large areas. This is termed "granular ophitic orthopyroxene" in Appendix I. Simultaneous with this gradual change in the texture of the hypersthene there is an increase in the amount of exsolved blebs of augite (Fig. 36), but this amount remains considerably less than in the inverted pigeonite at higher levels. The texture of this hypersthene corresponds closely to the typical units of similarly orientated cumulus grains of inverted pigeonite (to be discussed in the ensuing section) except for the difference in the amount of exsolved augite. Small quantities of inverted pigeonite persist in these rocks. Only at about 2300m above the Merensky Reef does the exsolved augite in the hypersthene correspond to the quantities typical of inverted pigeonite.

From the observed textural relationships it seems as though there is a gradual transition from ophitic primary hypersthene to inverted pigeonite. This is apparent from the gradually increasing amounts of exsolved augite. Over this entire transition zone, pigeonite also crystallized from the magma. A possible explanation for the coexistence of inverted pigeonite and primary hypersthene, as well as for the observed textural features in this "transition zone" is given further below (p. 83).

b) Units of similarly orientated grains of inverted pigeonite

All the gabbroic rocks of the Bushveld Complex which contain cumulus grains of inverted pigeonite are characterized by the occurrence of this mineral as groups of grains which possess similar orientations over large areas. These grains of inverted pigeonite usually contain two sets of exsolution-lamellae of augite. One set has the same orientation in each grain throughout the group or unit of inverted pigeonite grains, whereas the orientation of the second set of

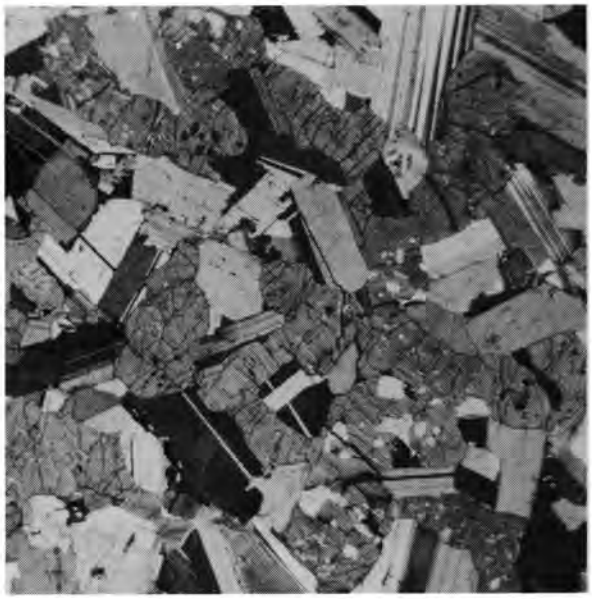

Fig. 36. Similarly orientated crystals of orthopyroxene (grey) which contain a few blebs of exsolved augite. G589, Uysedoorns 47 JT. Crossed nicols, x20.

Fig. 37. Several grains of orthopyroxene (in extinction) which together contain five sets of pre-inversion exsolution-lamellae of augite orientated at random and one set of post-inversion exsolution-lamellae of augite parallel to the (100) plane of the orthopyroxene. L13, Mineral Range 190 JS, Crossed nicols, x35. (Taken from Von Gruenewaldt, 1970, Fig. 1, p. 67).

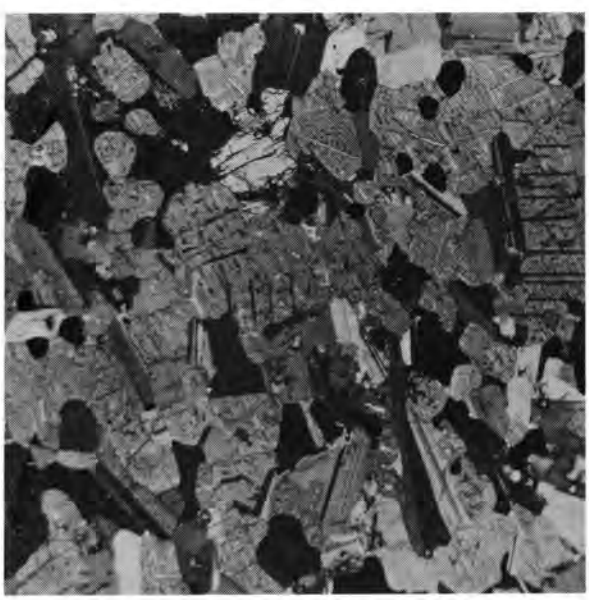

Fig. 38. A group of similarly orientated grains of orthopyroxene (grey) which contain pre- and post-inversion exsolution-lamellae of augite. G314, Luipershoek 149 JS. Crossed nicols, x20.

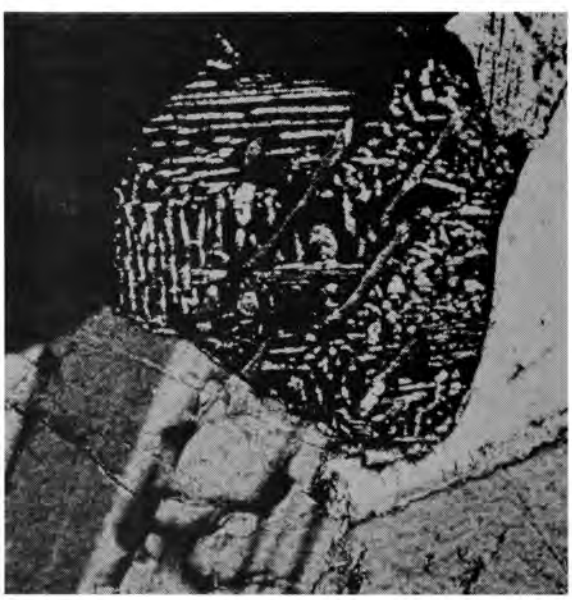

Fig. 39. A grain of inverted pigeonite (in extinction) which contains two sets of post-inversion exsolution-lamellae of augite. Horizontal lamellae parallel to (100), vertical lamellae parallel to (001), diagonal lamellae exsolved prior to inversion. G460, Mapochsgronde 500 JS. Crossed nicols, x75.

exsolution-lamellae differs from grain to grain in the same unit (Fig. 37). It was found without exception that the former set of exsolved lamellae of augite is orientated parallel to the (100) plane of the orthopyroxene host and that the latter set of exsolution-lamellae, which are usually much broader, is orientated at random in the orthopyroxene.

Augite usually exsolves as lamellae parallel to the (001) plane in pigeonite. According to Poldervaart and Hess (1951, p. 482), these lamellae are retained after inversion to orthopyroxene along a relict (001) plane, a plane near to (101) in the orthopyroxene. Bruynzeel (1957, p. 509) found that these pre-inversion exsolution-lamellae lie closer to the (102) plane of the orthopyroxene. This was not observed in the thin sections investigated from the Bushveld Complex, where most of the pre-inversion exsolution-lamellae of augite are orientated at random in the orthopyroxene.

Fortunately, the author had at his disposal the sections which were prepared for petrofabric analyses by Van den Berg (1946, p. 155). Two different types of stereographic plots were made from the majority of his sections. Firstly, the pre-inversion exsolution-lamellae were plotted with respect to the igneous layering (Fig. 40) and secondly, with respect to the orthopyroxene host (Fig. 41).

From Fig. 40, a compilation of a-, b- and c- petrofabric diagrams (see Van den Berg, 1946, p. 160), it can be seen clearly that the majority of the pre-inversion exsolution-lamellae have an orientation nearly perpendicular or perpendicular to the plane of igneous layering. Taking into consideration that these lamellae exsolved parallel to the (001) plane in pigeonite it is evident that most of the pigeonite grains represent settled crystals which came to rest on the magma floor with their major crystallographic axis (c-axis) parallel to the igneous layering.

Fig. 41 represents a compilation of a number of stereograms on which the pre-inversion exsolution-lamellae were plotted together with the optical orientation of the orthopyroxene host. This figure illustrates the random orientation of the pre-inversion exsolution-lamellae of augite in the inverted pigeonite. The tendency of these lamellae to be concentrated along a certain zone in the orthopyroxene cannot be ascribed to rules governing the inversion of pigeonite to orthopyroxene. Seeing that these plots represent the poles of the exsolution-lamellae, which, as stated in the previous paragraph, are orien-

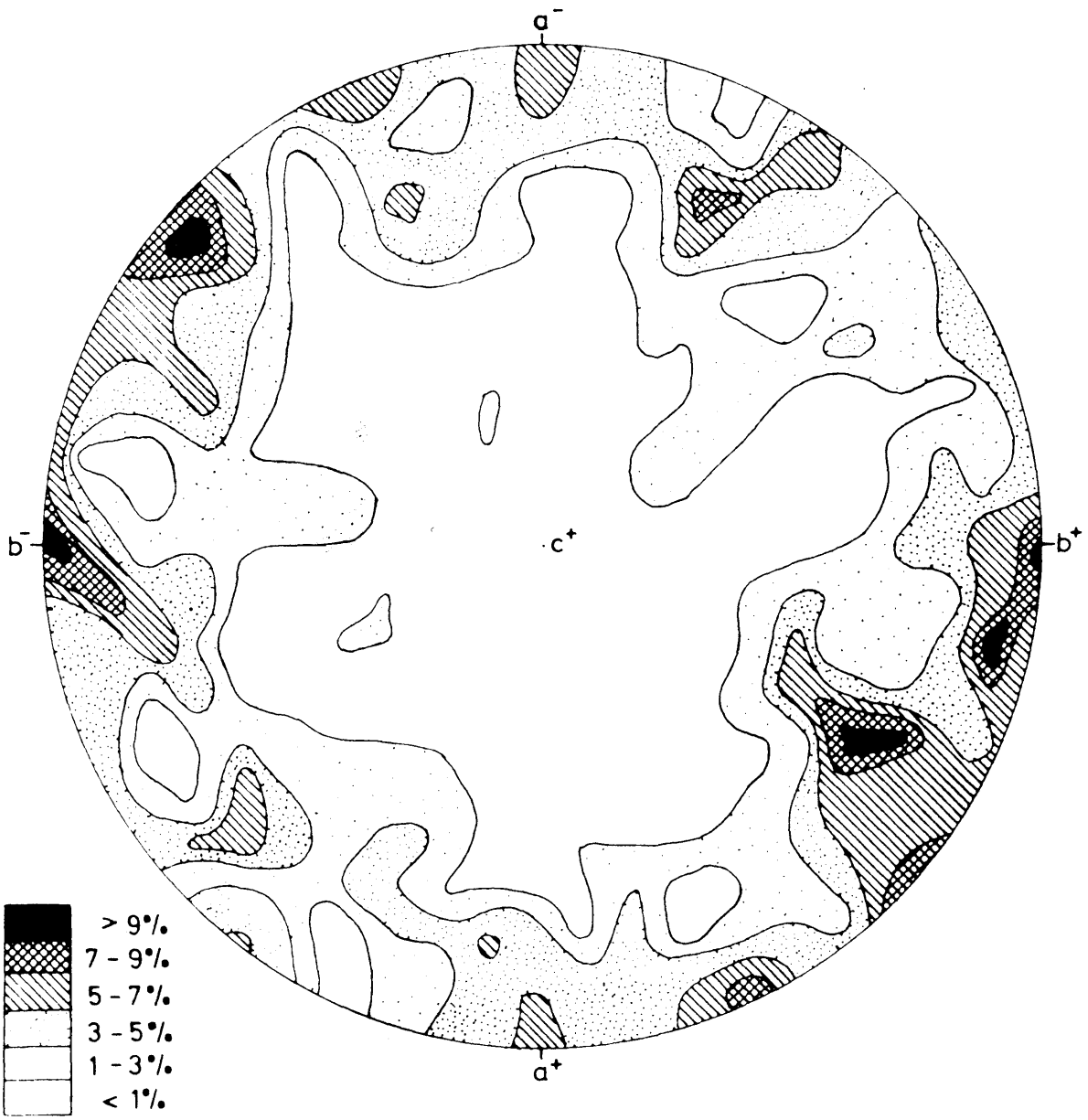

Fig. 40. Contoured distribution diagram of 227 pre-inversion exsolution-lamellae of augite in orthopyroxene, from Van den Berg's thin sections cut perpendicularly to the a, b and c fabric axes, a^+-a direction of dip, b^+-b^- strike, c^+-perpendicularly to layering.

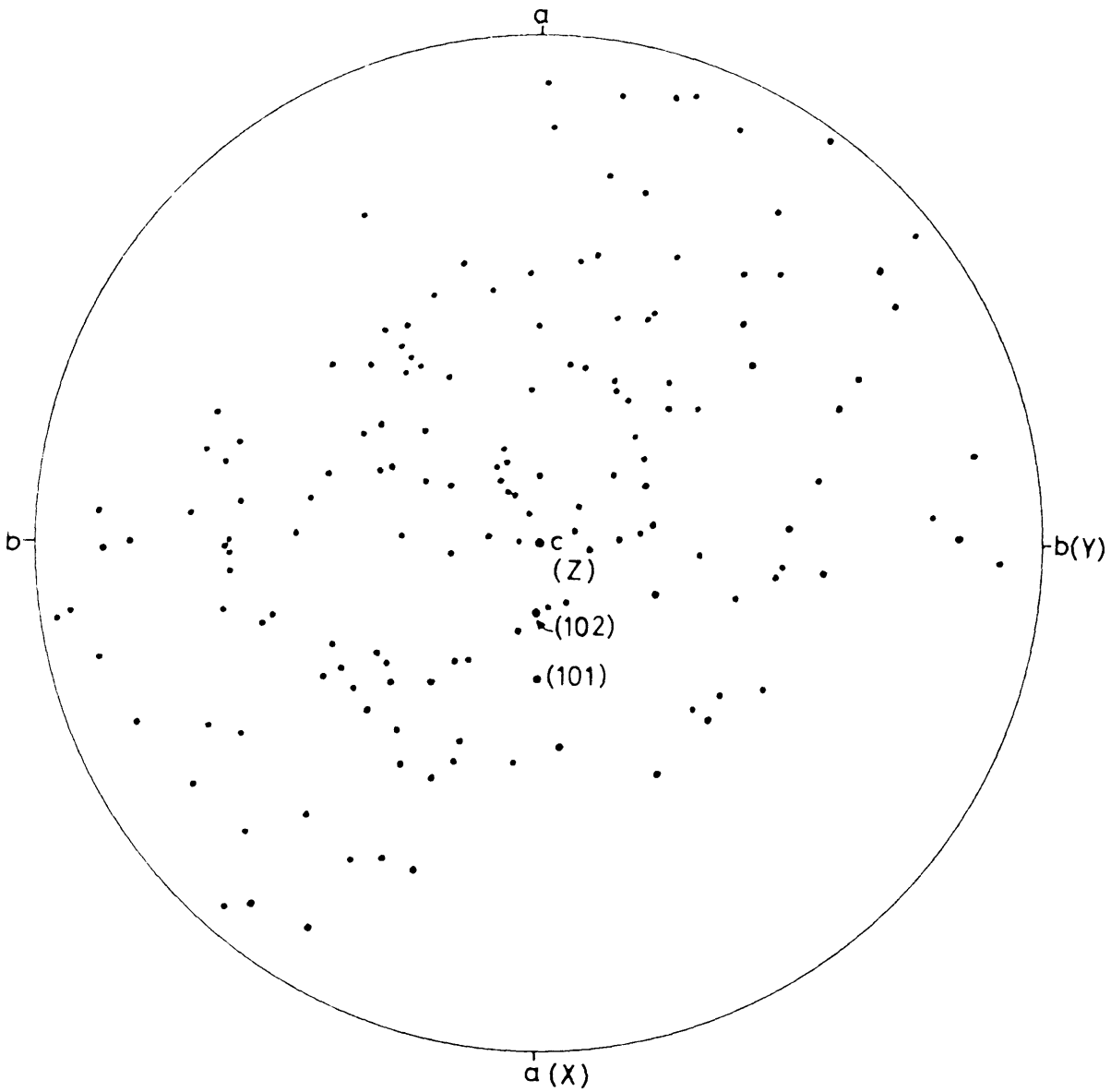

Fig. 41. Orientation of 149 pre-inversion exsolution-lamellae of augite in orthopyroxene from a number of Van den Berg's thin sections.

tated nearly perpendicular or perpendicular to the plane of layering, and seeing that the inverted pigeonites, although in groups, are orientated so that their major crystallographic axis lies close to or in the plane of layering (Van den Berg, 1946, p. 176, Fig. 18) a concentration of lamellae along a certain zone in the orthopyroxene is to be expected.

According to Poldervaart and Hess (1951, p. 482) the inversion of pigeonite to orthopyroxene develops in such a way that the b and c crystallographic axes of the parent-pigeonite are retained in the orthopyroxene. They do, however, describe exceptions to this rule. From Fig. 37 and from several other sections investigated from all over the Bushveld Complex, it seems as though the orientation of the inverted pigeonite bears no relation to that of the primary phase. This is not peculiar to the Bushveld Complex; it has been recorded from the Skaergaard Intrusion (Brown, 1957, p. 532-534), from Insizwa (Bruynzeel, 1957, p. 513) and from Ingeli (Maske, 1964, p. 61).

The same phenomenon was observed by Bowen and Schairer (1935, p. 151) who investigated the inversion relationship of orthopyroxene on heating. They found that orthopyroxene approaching the two end-members of the $MgSiO_3$-$FeSiO_3$ series are transformed readily into the monoclinic modification, whereas the intermediate members are only transformed with the aid of a flux and that "in general, a single crystal or crystal fragment of the orthorhombic pyroxene is transformed into an aggregate of several grains of monoclinic pyroxene of random orientation with respect to each other and to the original orthorhombic substance" (ibid., p. 169). They ascribe the sluggishness of the inversion of the intermediate members to structural complexities and to the steady decline in the inversion temperature with enrichment in iron.

Brown (1967, p. 351), who investigated experimentally the inversion relationship of pigeonite and orthopyroxene on natural, inverted pigeonites, found that in the absence of a flux the inversion was sluggish and that the reaction took place over a long period of time at elevated temperatures. In the presence of a liquid of composition similar to that of the magma from which the investigated natural pyroxenes had crystallized, the inversion took place readily, and at much lower temperatures than in the absence of liquid.

As mentioned previously, the groups of grains of inverted pigeonite possess the same optical orientation over large areas (Fig. 38). The grains of each group extinguish simultaneously or very nearly so, but differ in orientation

from grains of another group. This was previously observed in gabbroic rocks from the Bushveld Complex by B. V. Lombaard (1934, p. 26), Van den Berg (1946, p. 176), A. F. Lombaard (1949, p. 353), Raal (1965, p. 16) and Von Gruenewaldt (1966, p. 84) as well as by Maske (1964, p. 61) in similar rocks from the Ingeli Mountain Range. The size of these units varies considerably, but may attain a diameter of a few centimetres. Van den Berg (1946, p. 178) counted as many as 80 individual grains, in one thin section, all belonging to the same group.

To explain the random orientation of the pre-inversion exsolution-lamellae of augite in inverted pigeonite groups from Ingeli, Maske (1964, p. 61) suggests that, owing to the sluggishness of the structural rearrangement, inversion did not take place at the appropriate temperature. He is of the opinion that primary hypersthene was one of the first minerals to be precipitated from the interstitial liquid around the grains of pigeonite below the inversion temperature and thus formed rims free from lamellae. This stable orthorhombic phase would then start the inversion of the pigeonite in such a manner that the orientation of the secondary orthopyroxene would be continuous with the mantles of late hypersthene. This explanation is not applicable to the units of inverted pigeonite in the Bushveld Complex because of the absence of mantles of orthopyroxene free from lamellae, and because the units seem to have common orientations with their crystallographic c-axes parallel to the plane of igneous lamination.

It seems obvious that before inversion the orthopyroxene units consisted of several cumulus crystals of pigeonite. On cooling, lamellae of augite were exsolved parallel to the (001) plane of each pigeonite grain. When the inversion temperature was reached, directed pressure due to the accumulating superincumbent mass developed, and the first pigeonites to invert were probably those which, after inversion, produced an orthopyroxene with an orientation most stable under the prevailing conditions of pressure. This was not difficult to achieve, because many of the pigeonite crystals were favourably orientated (Fig. 40). All the grains with different orientations would take longer to invert owing to the sluggishness of inversion which probably took place in the absence of a flux, i. e. after most of the intercumulus liquid had already crystallized. As the pigeonite grains were probably in contact with one another, the first-formed orthopyroxene could set off the inversion in the adjoining grains, which would adopt an orientation continuous with that which started the reaction. This

process would then continue until all the pigeonite grains were inverted and this would result in groups of similarly orientated grains of inverted pigeonite which contain pre-inversion lamellae of augite orientated at random. On further cooling, more augite was exsolved parallel to the (100) plane of the inverted pigeonite. These post-inversion exsolution-lamellae of augite therefore have the same orientation throughout a unit. In a few sections a second set of post-inversion exsolution-lamellae was observed (Fig. 39) and is exsolved parallel to the (001) plane of the inverted pigeonite.

A. F. Lombaard (1949, p. 353 and Fig. 2) describes several adjacent grains of inverted pigeonite of different orientation. They contain parallel pre-inversion exsolution-lamellae of augite with the same optic orientation, which pass from one grain into another. In this case, a single grain of pigeonite evidently produced on inversion several grains of orthopyroxene of different orientation. This has also been observed in some of the thin sections investigated by the author, but is not very common. It seems as though the inversion was not always influenced by directed pressure from the accumulating crystal mass which might be due to a very stable framework of feldspar crystals.

5. The phase-change from orthopyroxene to pigeonite

The application of the experimentally observed relationships in the pyroxene quadrilateral to natural pyroxenes revealed important information on the crystallization trends during fractionation of a basaltic magma. In this regard, the early work of Hess (1941) and of Poldervaart and Hess (1951) is noteworthy. These authors showed that particular exsolution textures in the pyroxenes could be related to various stages of fractional crystallization, and Brown (1957, p. 527) related these exsolution textures to the cooling history of the Skaergaard magma.

Hess (1941, p. 583 and 1960, p. 40) and Brown (1957, Fig. 5, p. 530) related the inversion curve of Bowen and Schairer (1935) to crystallization temperatures of natural pyroxenes in the Bushveld, Stillwater and Skaergaard Intrusions. Yoder and Tilley (1962, p. 390-391) and Yoder and others (1963, p. 90) have shown that, owing to the uncertainty of the nature of the inversion, inversion temperature, pressure effects and the uncertainty of the influence of the $CaSiO_3$ component, magma temperatures cannot be estimated from the orthopyroxene-clinopyroxene inversion.

Recently, Brown (1967, p. 451) has reinvestigated the inversion relation-

ships of natural pyroxenes in the presence of andesitic liquid. He found that a pigeonite from the Bushveld Complex with composition $En_{40}Fs_{60}$ (wt. per cent) crystallized from a liquid of ferrodioritic composition at between 1050^{o} and $1060^{o}C$ at atmospheric pressure. This inverted pigeonite (S. A. 616) was collected by Atkins (1969, p. 232) from Subzone B of the Upper Zone, probably at a horizon between the uppermost magnetitite seam (No. 7) of Subzone B and the base of Subzone C. Inversion of this pigeonite to the orthorhombic phase took place at $1000^{o}C$, at atmospheric pressures and would correspond to an inversion temperature of $\pm$ $1025^{o}C$ at a pressure of 3-4 Kb (Brown, 1967, Fig. 10, p. 350) which is an estimate for this level in the intrusion.

Owing to the uncertainty which prevailed prior to detailed studies of the Main Zone (Molyneux, 1970 and this investigation) about the composition and the height in the intrusion at which pigeonite appears in the sequence, a number of specimens was collected by the author early in 1968 along a road which traverses the Main Zone on Dsjate 249 KT in the Leolo Mountains (Fig. 42). These samples were supplemented by those collected by Dr. L. Liebenberg along the same road.

Five samples of orthopyroxene from the Dsjate traverse were analysed by the National Institute for Metallurgy. The results as well as the structural formulae and the Fe:Ca:Mg ratios are given in Table III. The Fe:Ca:Mg ratios of these new analyses, as well as those of previously published analyses (Table IV) are plotted on Fig. 43 on which the trend of crystallization of Ca-poor pyroxenes was inferred from these analyses and from optical determinations of orthopyroxenes which were not analysed. The thin dotted lines on this diagram are not tie-lines between coexisting pairs of Ca-poor pyroxenes, but are the minimum and maximum Fe/Mg ratios at which primary hypersthene and inverted pigeonite were found to coexist in the rocks from Dsjate and from the area investigated in this study. The Fe/Mg ratio was derived in both instances from the more abundant primary hypersthene.

The results obtained from the study of the rocks from Dsjate were substantiated by the study of the rocks from the Roossenekal area (see p. 68). On Dsjate cumulus orthopyroxene (G10) is replaced by ophitic orthopyroxene (G9) about 750m above the Merensky Reef.

Ophitic orthopyroxene was found to be the only Ca-poor pyroxene up to a Mg:Fe ratio of 63:37, but at a higher Mg:Fe ratio small crystals of inverted

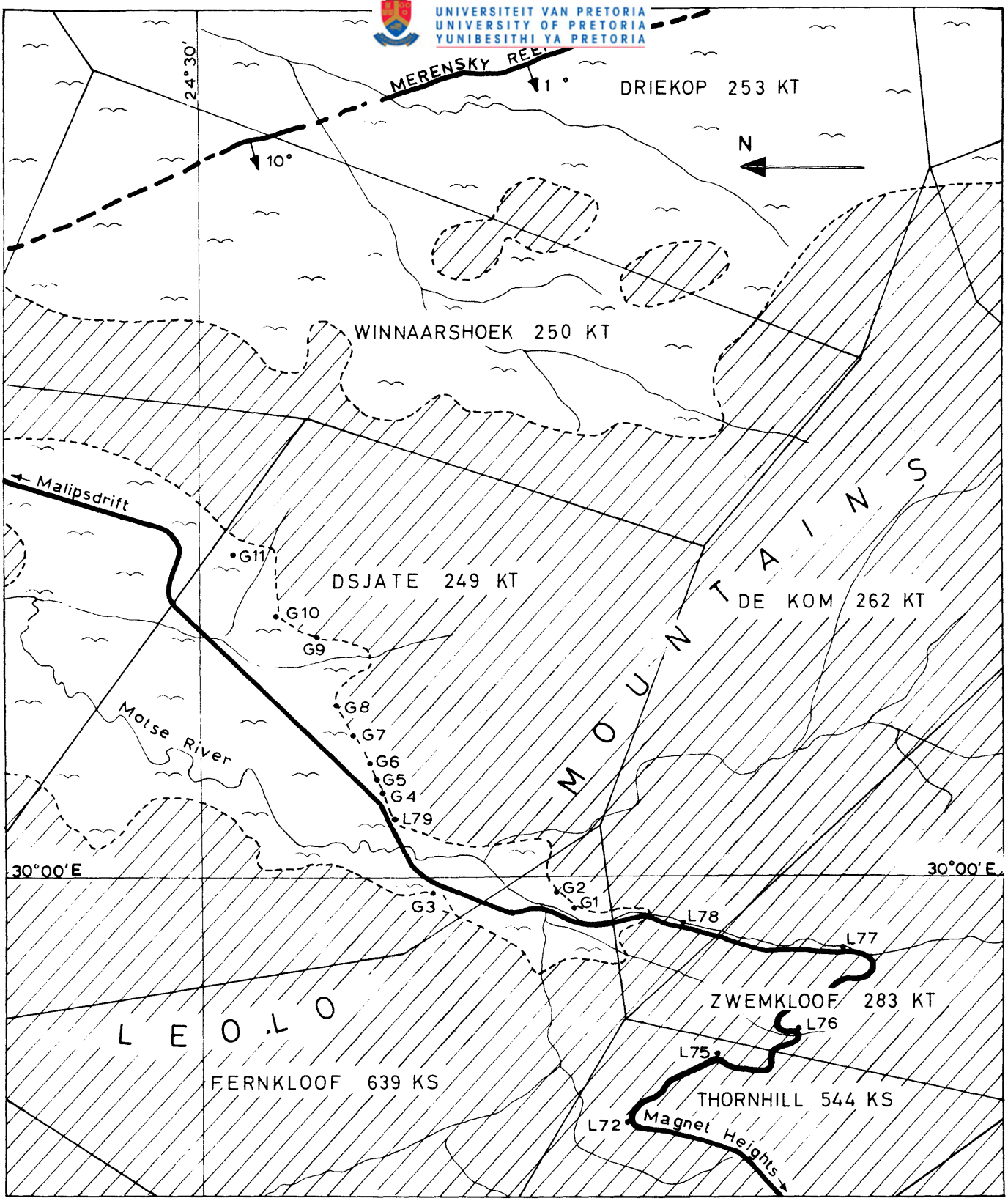

FIG. 42. MAP SHOWING LOCALITIES OF SAMPLES COLLECTED ON DSJATE 249 KT AND VICINITY

SCALE 1:50 000

TABLE III CHEMICAL ANALYSES AND STRUCTURAL FORMULAE OF ORTHOPYROXENE FROM THE EASTERN TRANSVAAL

		G10	G8	G7	G6	L77
	SiO_2	53, 71	53, 93	53, 04	52, 83	53, 34
	TiO_2	0, 25	0, 42	0, 30	0, 30	0, 30
	Al_2O_3	1, 33	1, 30	1, 38	1, 41	1, 52
	Fe_2O_3	1, 37	1, 31	1, 71	1, 52	1, 69
	FeO	16, 05	15, 43	17, 05	18, 12	16, 23
	MnO	0, 36	0, 40	0, 43	0, 44	0, 46
	MgO	25, 03	25, 06	24, 15	23, 20	23, 14
	CaO	1, 10	1, 39	1, 19	1, 35	2, 60
	Na_2O	0, 47	0, 55	0, 39	0, 43	0, 54
	K_2O	0, 10	0, 09	0, 09	0, 08	0, 08
	H_2O	n. d.	n. d.	n. d.	n. d.	n. d.
		99, 77	99, 88	99, 73	99, 68	99, 90
	Atomic per cent					
	Ca	2, 3	2, 8	2, 4	2, 7	5, 3
	Mg	70, 0	70, 4	67, 6	65, 7	65, 6
	*Fe	27, 7	26, 8	30, 0	31, 6	29, 1
	Numbers of ions on the basis of 6 oxygens					
Z	Si	1, 959	1, 961	1, 948	1, 953	1, 956
Z	Al	0, 037	0, 036	0, 049	0, 044	0, 044
WXY	Al	0, 021	0, 021	0, 012	0, 018	0, 022
WXY	Fe^{3+}	0, 038	0, 035	0, 048	0, 041	0, 048
WXY	Fe^{2+}	0, 489	0, 469	0, 524	0, 560	0, 497
WXY	Mn	0, 014	0, 013	0, 014	0, 014	0, 014
WXY	Mg	1, 360	1, 358	1, 322	1, 277	1, 264
WXY	Ca	0, 044	0, 054	0, 046	0, 053	0, 101
WXY	Na	0, 032	0, 039	0, 026	0, 029	0, 039
WXY	K	0, 004	0, 004	0, 004	0, 004	0, 004
WXY	Ti	0, 008	0, 011	0, 009	0, 009	0, 009
	Z	1, 996	1, 997	1, 997	1, 997	2, 000
	WXY	2, 010	2, 004	2, 005	2, 005	1, 998

*Fe = Fe^{3+} + Fe^{2+} + Mn

TABLE III (continued)

G10 Hypersthene from norite, 700m above Merensky Reef. Dsjate 249 KT, Lydenburg district.

Analysis corrected for 1,5% augite of composition $Wo_{41}En_{44}Fs_{15}$.

G8 Hypersthene from norite, 850m above Merensky Reef. Dsjate 249 KT, Lydenburg district.

Analysis corrected for 1,18% augite of composition $Wo_{41}En_{44}Fs_{15}$.

G7 Hypersthene from hypersthene gabbro, 950m above Merensky Reef, Lydenburg district.

Analysis corrected for 0,87% augite of composition $Wo_{40,5}En_{42}Fs_{17,5}$

G6 Hypersthene from norite 1000m above Merensky Reef, Lydenburg district.

Analysis corrected for 0,57% augite of composition $Wo_{41,5}En_{41,5}Fs_{17}$

L77 Pigeonite inverted to hypersthene from fine-grained norite 1600m above Merensky Reef, Zwemkloof 283, KT, Lydenburg district. No impurities.

Analyses by the National Institute for Metallurgy, Johannesburg.

TABLE IV Ca:Mg:Fe RATIOS OF BUSHVELD ORTHOPYROXENE FROM PREVIOUSLY PUBLISHED ANALYSES

	1a	2a	3a	4a	5a	6a	7a	8a
Ca	2,8	3,1	2,3	2,8	2,2	2,9	8,4	7,6
Mg	85,0	83,3	75,0	77,7	72,0	60,4	55,4	40,7
Fe	12,2	13,6	22,7	19,5	25,8	36,7	36,2	51,7

1a Cumulus bronzite from bronzitite (7666) of the Basal Zone, Jagdlust. (Hess, 1960, p. 25).

2a Cumulus bronzite from bronzitite (S. A. 685) of the Basal Zone, Jagdlust (Atkins, 1969, p. 231).

3a Cumulus bronzite from gabbro (S. A. 660) of the Critical Zone, Jagdlust (Atkins, 1969, p. 231).

4a Cumulus bronzite from gabbro (S. A. 722) of the Critical Zone, Jagdlust (Atkins, 1969, p. 231).

5a Cumulus bronzite from gabbro (S. A. 733) of the Main Zone, Middelpunt (Atkins, 1969, p. 231).

6a Cumulus inverted pigeonite (S. A. 738) of the Main Zone, Blauwbloemetjeskloof (Atkins, 1969, p. 231)

7a Cumulus inverted pigeonite (7493) of the Main Zone, Pretoria district (Hess, 1960, p. 28)

8a Cumulus inverted pigeonite from ferrogabbro (S. A. 616), Upper Zone near Magnet Heights (Atkins, 1969, p. 231).

pigeonite are also developed. These two phases were found to coexist in specimens G2-G4, over 300m, and at a Mg:Fe ratio of approximately 65:35, pigeonite is the only Ca-poor phase present.

Although the position of L77 in Fig. 43 seems anomalous as this rock is from a stratigraphical position some 300m above the level at which primary hypersthene disappears, it indicates that pigeonite with a Mg:Fe ratio of 69:31 was precipitated from the magma and also that the more magnesian pigeonites contain less of the $CaSiO_3$ component than the more iron-rich varieties. This low Fe/Mg ratio for pigeonite may be explained in a similar way as that of the fine-grained norite underlying the Pyroxenite Marker in the Roossenekal area (see p. 88).

6. Coexisting inverted pigeonite and primary hypersthene

It has been recorded above that in parts of Subzones B and C of the Main Zone inverted pigeonite coexists with primary ophitic hypersthene. This association seems anomalous because experimental studies in the $CaSiO_3$ - $MgSiO_3$ - $FeSiO_3$ system on synthetic as well as natural pyroxenes (Bowen and Schairer, 1935, Yoder et al., 1963, p. 88-91; Brown 1967, p. 347) have shown that an inversion relationship exists between pigeonite and hypersthene. The temperature of this inversion drops with increase in the Fe-content of the Ca-poor pyroxene, and as a result of fractional crystallization of a basaltic magma the crystallization curve of the Ca-poor pyroxenes intersects the inversion curve at a specific Mg:Fe ratio which depends on the composition of the magma. If the magma is therefore in equilibrium with the crystallizing phases, as is generally assumed for slowly cooling intrusions like the Bushveld, then either primary hypersthene or pigeonite coexists with augite, but not both. Where non-equilibrium conditions prevailed, as during rapid crystallization in basaltic or andesitic lavas as well as in dolerites and diabases, primary orthopyroxene and pigeonite may be present in the same rock.

Recently, however, Nakamura and Kushiro (1970a, p. 275 and 1970b,

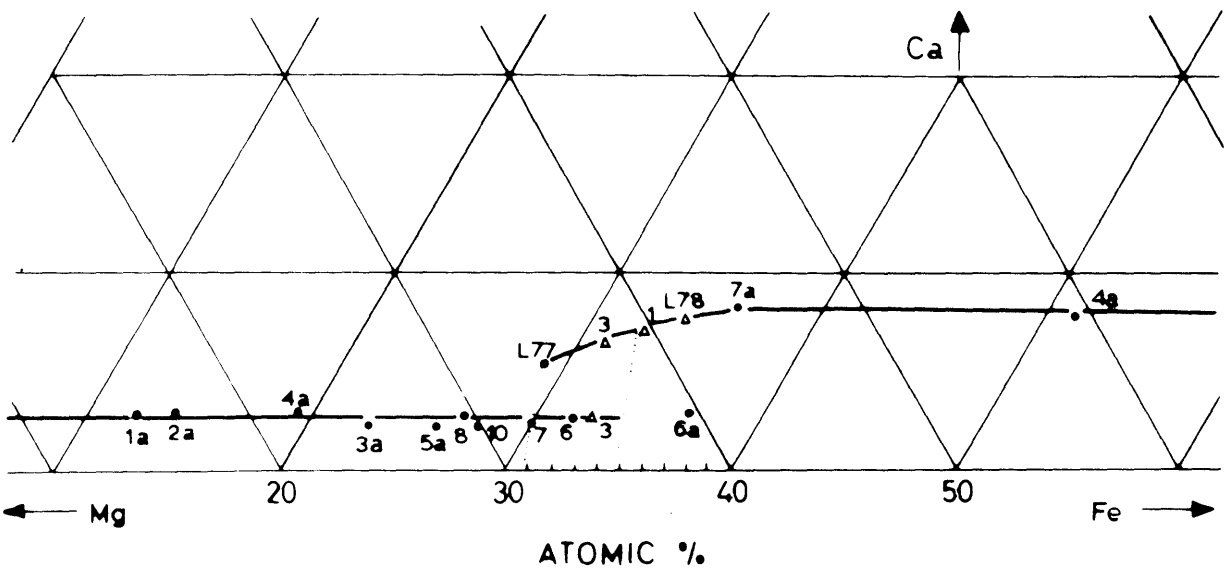

Fig. 43. Trend of Ca-poor pyroxenes from the Bushveld Complex. (Triangles denote that compositions were inferred from optical data.)

p. 2012-2014) have shown from textural relationships and chemical analyses of coexisting pyroxenes that the so-called "inversion interval" (Kuno and Nagashima 1952, p. 1001) between orthopyroxene and pigeonite is actually a hypersthene-pigeonite tie-line of the three-phase triangle augite-hypersthene-pigeonite. With the aid of their diagram (1970b, Fig. 11, p. 2013) reproduced here in a modified version as Fig. 44, it is possible to explain the coexistence of hypersthene and pigeonite in slowly cooled intrusions like the Bushveld.

Fig. 44b is the pyroxene quadrilateral in which the crystallization trends of Bushveld pyroxenes are indicated. The trend for the Ca-rich pyroxenes is after Atkins (1969, Fig. 3, p. 239) whereas the trend for the Ca-poor pyroxenes is based on the chemical analyses by Atkins (1969) and on this investigation (Fig. 43). Tie-lines between coexisting hypersthene, pigeonite and augite are hypothetical, although the positions of the hypersthene points of the triangles are based on the lowest and highest Fe/Mg ratio determined for this mineral where it coexists with pigeonite. Fig. 44a is a temperature-composition diagram along the join $Ca_{8,5}Mg_{91,5}$(A) - $Ca_{8,5}Fe_{91,5}$(B). Two temperature curves ML-ML' and MS-MS' are indicated on Fig. 44a instead of only one on the original diagram by Nakamura and Kushiro. This was done because, with slow cooling of a magma, crystallization takes place over a certain temperature interval. ML and MS do not necessarily refer to the liquidus and solidus temperatures of the magma, but rather to an arbitrary temperature interval between the actual liquidus and solidus temperatures. In this figure pigeonite has a stability field at higher temperatures than augite plus hypersthene. These two fields are separated from each other by a three-pyroxene region, the temperature of which decreases with increasing Fe/Mg ratio (Nakamura and Kushiro, 1970, p. 2012).

To the left of point p in Fig. 44a, hypersthene and augite crystallized from the Bushveld magma. When ML, which may be taken as the crystallization temperature of Ca-poor pyroxene, reached point p, the magma moved into the stability field of hypersthene + augite + pigeonite, with the result that pigeonite (Fe/Mg ratio of x) crystallized. Some of this pigeonite might have formed as a result of the reaction hypersthene + liquid $\rightleftharpoons$ pigeonite (ibid., p. 2014). A slight drop in temperature to MS (at the same Fe/Mg ratio as ML at p) would result in these pigeonite crystals coming into contact with magma which was in the stability field of hypersthene and augite. Immediate inversion of the early

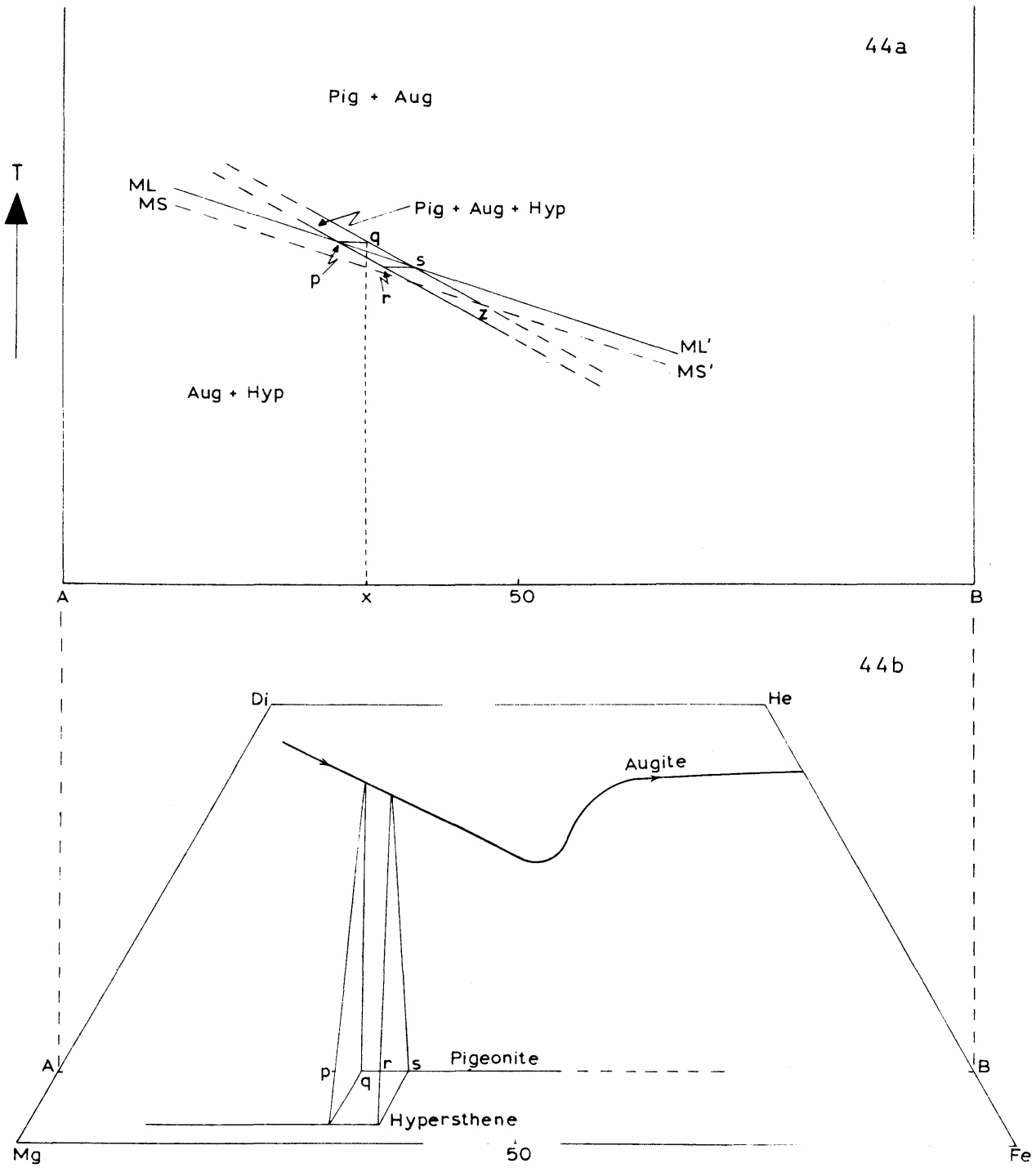

FIG. 44. SCHEMATIC DIAGRAM SHOWING THE CRYSTALLIZATION OF PYROXENES IN THE BUSHVELD COMPLEX. FOR EXPLANATION SEE TEXT. (ADAPTED FROM NAKAMURA AND KUSHIRO 1970, p. 2013)

pigeonite would be the result, but seeing that the Fe/Mg ratio of q is larger than that of the hypersthene and augite crystallizing in equilibrium with the magma, this would effect the dissolution of the early pigeonite. This could bring about the enrichment of the magma in the constituents of hypersthene after a considerable amount of plagioclase and augite had already crystallized, and could cause the large ophitic hypersthene crystals. Small, early pigeonite crystals (now inverted to orthopyroxene) could escape complete dissolution by being enclosed in augite. This is seen by the irregular shape of the former when enclosed in the latter.

As fractional crystallization of the magma continued, the composition of the liquid changed along ML towards s. This resulted in a decrease in the difference between the Fe/Mg ratio of the magma and the early crystallizing pigeonite. Consequently, the temperature interval between MS and the stability field of the augite + hypersthene + pigeonite was gradually reduced, with the result that the time interval available for complete dissolution of the early inverted pigeonite was also reduced. This might have resulted in reaction between magma and pigeonite to form hypersthene. As a result of this reaction, the exsolved augite in the early pigeonite could have been expelled during equilibration of Fe/Mg ratios of the magma and the inverted pigeonite.

As the Fe/Mg ratio of early pigeonite and of the crystallizing magma decreased further, equilibration of early pigeonite by reaction with liquid to form hypersthene continued, but gradually more and more of the augite exsolved from pigeonite was retained owing to a decrease in the reaction time. It seems therefore, that the transition from pigeonite to hypersthene changed from complete dissolution by the magma to reaction with the magma, and hence the texture also changed from ophitic hypersthene to grains, optically continuous over large areas enclosing only a few blebs of exsolved augite. This reaction was replaced by inversion proper as ML moved into the stability field of pigeonite at point s and MS moved into the stability region augite + hypersthene + pigeonite. Where these conditions prevailed, late hypersthene mantles around pigeonite grains could be held responsible for the units of similarly orientated grains of inverted pigeonite as proposed by Maske (1964, p. 61) for the origin of this texture in rocks from the Ingeli Mountains, and also for the lamellae-free rims of inverted pigeonite observed by Brown (1957, p. 528) from Skaergaard. As soon as MS reached point z pigeonite would be the only Ca-poor pyroxene to be precipitated from the magma.

A way in which to determine whether a mechanism as proposed above was operative in giving rise to coexisting inverted pigeonite and primary hypersthene, would be to determine the Fe/Mg ratio of these two, because, according to the above hypothesis, the inverted pigeonite should have a higher Fe/Mg ratio than the coexisting hypersthene. As it is not possible to separate sufficient quantities of the two phases from the same rock, especially inverted pigeonite, electron microbe analysis would be the only way in which to determine the differences in Fe/Mg ratio.

The fine-grained norite directly below the Pyroxenite Marker contains inverted pigeonite only, with composition Fs_{32}, and should according to the above hypothesis contain both Ca-poor phases. A rise in temperature of the magma at this level in the intrusion would have the effect that point s in Fig. 44a would move to lower Fe/Mg ratios. Simultaneously, a change in the composition of the magma was probably brought about by a small influx of fresh magma, prior to larger quantities being added which resulted in the crystallization of primary hypersthene from the Pyroxenite Marker onwards. The composition of the pigeonite in the fine-grained norite L77 from Dsjate (see above) may be explained in a similar way.

B. PLAGIOCLASE

1. Determinative methods

The An content of the plagioclase feldspars was determined by means of X-ray powder data, 2V, Eulerian angles and extinction angles. As a result, several values are given in Appendix I and generally the value which corresponds most closely to the average was used to construct the mineral variation curves of Folder III.

a) X-ray determinations

Desborough and Cameron (1968, p. 117) have established that the plagioclases of the Bushveld Complex are of the low temperature structural variety and consequently X-ray powder diffraction patterns of plagioclases, especially in the range An_{50} - An_{75}, are useful in the determination of the An content (Smith and Gay 1958, p. 760). Various combinations of lines are used by different authors to determine the composition of the plagioclase feldspars. Smith and Gay (1958, p. 744-762) recommend the value $2\Theta_{131} + 2\Theta_{220} - 4\Theta_{1\bar{3}1}$, but Desborough and Cameron (1968, p. 120) have shown that the curve for $2\Theta_{131} + 2\Theta_{220} - 4\Theta_{1\bar{3}1}$ gives values between 2-5 mol. per cent An too high in

the compositional range $An_{60} - An_{80}$. In this study, X-ray powder patterns were obtained by using an AEG Guinier camera developed by Jagodzinski with Cu-$K\alpha_1$ radiation and silicon as internal standard. For the determination of the An content of the plagioclase the values $2\theta_{131} - 2\theta_{1\bar{3}1}$ and $2\theta_{\bar{2}41} - 2\theta_{\bar{2}\bar{4}1}$ were used, as recommended by Tröger (1965, p. 744). The An content of the plagioclases was obtained from the curves of Bambauer et al. (1965) as reproduced in Tröger (1965, p. 748 and 749, Figs. 249 and 250). A potassium content of more than 1 mol. per cent orthoclase apparently lowers the $2\theta_{131} - 2\theta_{1\bar{3}1}$ value considerably, but does not seem to affect the $2\theta_{\bar{2}41} - 2\theta_{\bar{2}\bar{4}1}$ values (Tröger, p. 746 and 749).

In the compositional range $An_{76} - An_{65}$, there is a close agreement in the An values obtained from $2\theta_{131} - 2\theta_{1\bar{3}1}$ and $2\theta_{\bar{2}41} - 2\theta_{\bar{2}\bar{4}1}$. Below An_{65}, the An value determined from $2\theta_{\bar{2}41} - 2\theta_{\bar{2}\bar{4}1}$ is mostly 2-3 mol. per cent higher than that determined from the $2\theta_{131} - 2\theta_{1\bar{3}1}$ value. The reason for this may be due to the K-feldspar which is present in amounts greater than 1 mol. per cent orthoclase (Table V). In specimens where the anorthite content was determined from X-ray data as well as from Eulerian and extinction angles, it was found that the An values obtained from the last two methods agree more closely with the values deduced from $2\theta_{131} - 2\theta_{1\bar{3}1}$, than those deduced from $2\theta_{\bar{2}41} - 2\theta_{\bar{2}\bar{4}1}$.

b) Universal stage determinations

i) 2V measurements

Although the determination of the An content of plagioclase by means of optic axial angles is generally considered to be the least accurate of all the various universal stage methods of determination, the degree of accuracy is increased to some extent by the use of conoscopic illumination (Burri, Parker and Wenk, 1967, p. 203-205).

Grain mounts were made of all samples which were also used for X-ray diffraction determinations, and the 2V was measured under conoscopic illumination on 8 to 10 grains per sample. Only such grains were used which allowed direct measurement of both optical axes of the indicatrix. All the readings on the universal stage were corrected, using an approximated n_y value and the curves provided by Tröger (1959, p. 124).

In most of the samples the 2V measurements fluctuate between $\pm$ 2 and 3^o from the averaged value, but in some samples, fluctuations of up to $\pm 4^o$ were measured. The An values for the averaged 2V were read off from the curves

of J. R. Smith (1960, Plate XII) and these values are listed in Appendix I. The An values thus obtained differ, for most samples, not more than 2 mol. per cent from the values obtained by other methods and only rarely is the difference more than 4 mol. per cent. No An values were determined by this method for measured 2V's of less than 78^{o} because of the uncertainty of the deduced composition from these angles in the range An_{57}-An_{47}.

Of interest is, that the An values obtained from the curves of Smith (1960, Plate XII) agree much more closely with the values determined from X-ray and other methods, than the values obtained from the curve supplied by Burri, Parker and Wenk (1967, Plate XII) which gives An values of 3 mol. per cent too low for plagioclases which contain more than 50 mol. per cent anorthite.

ii) Extinction angles

Extinction angles were measured on albite and on combined albite-Carlsbad twins. When albite twinning alone was used, the stage was tilted so that the extinction angle $[n_x']$ (010)⊥[100] was measured. The An content was then read off the curve supplied by Burri, Parker and Wenk (1967, Plate XI). Wherever possible, extinction angles were measured on grains which exhibited combined albite and Carlsbad twinning. This type of twinning has the advantage that any combination of $[n_x']$ ^(010) angles can be measured, and that several sets of measurements can be made on the same grain. The An content was then determined from the curves given in Tröger (1959, p. 102). Extinction angles were measured on at least five different crystals per thin section and the An values listed in Appendix I are the average values obtained by these methods. These methods were used, together with the Eulerian angles for plagioclases of Subzones B, C and D of the Upper Zone, most of which fall in a compositional range where the composition cannot be determined by either 2V measurements or X-ray powder techniques or both. Extinction angles were also used to some extent for plagioclases of the Main Zone where there was some discrepancy in the An values as determined by X-rays and 2V measurements.

iii) Eulerian angles

Burri, Parker and Wenk (1967, p. 186) consider the determination of the composition of plagioclases with the aid of Eulerian angles as being "die exakte Typisierung eines Plagioklases für mineralogische Spezialstudien". In this study, only Eulerian angles of the first order (ibid., p. 41-43 and 117-133) were measured on Roc-Tourné (combined albite-Carlsbad) twins, and the composition

TABLE V CHEMICAL ANALYSES, STRUCTURAL FORMULAE AND MOLECULAR PERCENTAGES OF PLAGIOCLASE

		PB4389	G491	G422	G277
SiO_2		48, 61	51, 36	53, 62	56, 36
Al_2O_3		31, 54	29, 83	28, 84	26, 61
Fe_2O_3		0, 39	0, 52	0, 24	0, 26
FeO		0, 14	0, 22	0, 36	0, 50
MgO		0, 12	0, 12	0, 09	0, 05
CaO		15, 78	14, 16	11, 89	9, 69
Na_2O		2, 64	3, 22	3, 92	5, 60
K_2O		0, 22	0, 21	0, 36	0, 49
H_2O^+		0, 25	0, 22	0, 35	0, 50
H_2O^-		0, 05	0, 08	0, 08	-
		99, 74	99, 94	99, 75	100, 06
Number of ions on the basis of 32(O)					
Z	Si	8, 972	9, 407	9, 773	10, 211
Z	Al	6, 861	6, 430	6, 185	5, 683
Z	Fe^{+3}	0, 064	0, 070	0, 031	0, 035
X	Fe^{+2}	0, 020	0, 035	0, 057	0, 076
X	Mg	0, 029	0, 029	0, 020	0, 011
X	Ca	3, 122	2, 774	2, 320	1, 881
X	Na	0, 949	1, 148	1, 389	1, 959
X	K	0, 049	0, 046	0, 079	0, 107
Z		15, 90	15, 91	15, 99	15, 93
X		4, 16	4, 03	3, 87	4, 03
Mol.%	An	75, 8	69, 9	61, 2	47, 7
Mol.%	Ab	23, 0	28, 9	36, 7	49, 6
Mol.%	Or	1, 2	1, 2	2, 1	2, 7

PB 4389 from norite, bore-hole PB1, Pietersburg 44JT.
6491 from fine-grained norite below the Pyroxenite Marker, Mapochsgronde 500 JT.
6422 from magnetite gabbro, Vlaklaagte 146 JS
6277 from magnetite anorthosite above Magnetite Seam 17 Onverwacht 148 JS.
Analyst: National Institute for Metallurgy, Johannesburg.

of the plagioclase was obtained from the chart given by Burri, et al. (1967, Plate I). Eulerian angles were usually obtained from only one grain per thin section. For most sections two sets of three angles (i.e. one set per twin) were measured on the stereographic projection and the composition given in Appendix I is therefore an average of six values.

2. Chemical analyses

Four samples of separated plagioclase were chemically analysed by the National Institute for Metallurgy. The object of these analyses was to give an indication of the accuracy of the composition as determined by optical means. Care was taken to ensure that the plagioclases were free of impurities by investigating this mineral in thin section prior to separation. This was necessary because, especially the plagioclases of the Upper Zone and those from rocks below the Pyroxenite Marker, contain tiny needles of magnetite. Comparison of these analyses (Table V) with those listed by Deer et al. (1963, Vol. 4, Tables 15 to 17, p. 115-118) shows them to have a slightly higher iron content, which may be ascribed to submicroscopic needles of magnetite.

From these analyses it would seem that optical determinations give An values of a few mole per cent lower than those calculated from chemical analyses (Table VI). Reverse zoning (Wager and Brown, 1968, p. 386) could be the cause of these differences, although special care was taken to ensure that plagioclase was separated from specimens which showed little or no zoning.

TABLE VI COMPARISON OF MOLECULAR ANORTHITE CONTENT OF PLAGIOCLASE AS DETERMINED BY DIFFERENT METHODS

Sample No.	PB4389	G491	G422	G277
Chemical analysis	76	70	61	48
Eulerian angles I	77	64	56	43
Extinction angles	76	65	56	44
2V	76	63	57	-
X-rays ($2\theta_{131}$-$2\theta_{\bar{1}31}$)	74	n. d.	57	-
n glass*	77	66	57	43

* Determined by A. Kleyenstüber and W. Dohmen.
n. d. - not determined.

3. Compositional variations

In general, the compositional trend, as indicated in Folder III resembles that of orthopyroxene very closely. The compositional breaks recorded in the orthopyroxene trend are also borne out by the plagioclase. The scatter of points in the plagioclase curve is however less, owing to the averaging of the An content as determined by several methods, and consequently the compositional trend as displayed by this mineral is considered to be more accurate than that of the orthopyroxene.

The An content of plagioclase is in the vicinity of 76 directly above the Merensky Reef and corresponds to the composition of this mineral in the reef (Wager and Brown, 1968, Fig. 192, p. 351; Molyneux, 1970, p. 33). Roux (1968, p. 70) on the other hand, recorded values varying between An_{73} - An_{85} for the Merensky Reef in the area a few kilometres to the east. At the first compositional break, 100m above the reef, the An content drops to 68, with a corresponding change in the Fs content of the coexisting inverted pigeonite. It is noteworthy that the change in composition of the Ca-poor pyroxene is much greater (14 mole per cent) than that of the plagioclase (9 mole per cent). Above this break, the composition of the plagioclase returns to above An_{70} for only a short distance, and then gradually drops to An_{64} at the bottom of the next compositional break at 1120m. Higher An values are only maintained for 100m above the break and from here onwards the composition changes progressively to An_{56} below the fine-grained norite which forms the top of Subzone B of the Main Zone.

In the fine-grained norite the composition of the plagioclase rises sharply to about An_{65} and this is analogous to the trend observed in the orthopyroxene. A possible explanation for this change is offered in the previous section on the orthopyroxene (p. 88). Above the Pyroxenite Marker, values of above An_{70} are maintained for about 350m before dropping rapidly to An_{60} at the top of the Main Zone.

The composition of the plagioclase fluctuates between An_{56} and An_{59} in the first 400m of the Upper Zone and drops to a fairly constant An_{53-55} for the greater part of Subzone C. In the top 100m of this subzone, the An content decreases to 50. Noteworthy is the change to An_{45} where cumulus apatite appears in the olivine diorites of Subzone D. The change in composition of the plagioclase at this level is not solely ascribed to a decrease in the Ca-content of the magma, but is considered to be partially due to the fact that fractionation led to the gradual

enrichment in the phosphorus content which reached saturation at this horizon and resulted in the crystallization of apatite. This caused a depletion of Ca in the magma and a consequent drop in the An content of the coexisting plagioclase.

In the lower 550m of Subzone D, cumulus apatite and plagioclase crystallized together, and owing to fractionation the composition drops gradually to An_{42}. The rocks between Magnetitite Seams 17 and 21, contain no apatite and as a result, the An content rises rapidly from 42 to 52, but where apatite appears again above the 21st Seam, the composition of the plagioclase drops to An_{45}, which is also the value obtained for the highest rock in this sequence where the composition could be determined. In the samples of the remaining 30m of the succession, the plagioclase feldspar is highly saussuritized, but in less altered samples, Atkins (1969, Fig. 1, p. 227) and Groeneveld (1970, Fig. 3, p. 40) found the composition to drop to An_{30} at the top of the intrusion.

4. Textural features

Not much attention was given to the textural features displayed by the plagioclase, as this necessitates a detailed study on its own, but the more important textures which were observed during the course of the investigation are briefly discussed below. Twinning is not included in the following discussions as no systematic evaluation was made of the frequency of types present. Molyneux (1970, p. 34) however, states that albite twinning is the most common in the Bushveld plagioclase.

a) Zoning

Zoning is present to some extent in practically all the thin sections investigated. During routine optical determinations of the composition of the plagioclase, the zoning of a few crystals was also determined and the observed values are given in Table VII. The zoning may be reversed, normal or oscillatory and is mostly confined to the outermost, usually narrow, rims of the crystals, but occasionally, especially when the zoning is oscillatory, the rims are wider. In the two specimens where oscillatory zoning was measured, the sequence is normal - reversed in the one and reversed - normal in the other. Specimen G351 (Table VII) requires special comment. The rock is an olivine gabbro from the base of Subzone C of the Upper Zone, and is characterized by the presence of a few small inclusions of anorthosite. The cumulus plagioclase of the rock exhibits reversed zoning from An_{53}-An_{63} whereas the plagioclase of the inclusion has a higher anorthite content and displays normal zoning from

An_{63}-An_{56}. Although the origin of the inclusions is uncertain, the observed zoning is probably inherent in the two rock types.

The recorded zoning in Table VII represents only a few routine determinations with the Universal Stage and much more detailed work is necessary to determine differences in An content between core and mantle of the plagioclase to deduce crystallization trends of the intercumulus liquid.

The presence of reversed zoning of the plagioclases in the rocks of the Bushveld Complex was remarked on by Wager and Brown (1968, p. 385-387) who found it to be unique to this intrusion. They reject the possibility of increased pressure on the confined pore spaces, as this mechanism would also have been operative in other intrusions. The alternative of an increase in pH_2O in the interstitial melt is favoured by them, as this would have the effect of lowering the liquidus - solidus temperatures in the anorthite - albite system. The outer parts of the cumulus crystals would attain equilibrium with this residual liquid by reaction and give rise to the more calcic rims. Simultaneously, SiO_2 would be released and result in the myrmekitic intergrowths commonly observed in plagioclases of the Bushveld Complex. However, myrmekite is not always present where plagioclase displays reversed zoning, as also noted by Ferguson and Wright (1970, p. 65) from rocks of the Critical Zone.

b) Bent crystals of plagioclase and interpenetration

Textural features indicative of deformation after deposition of the cumulus crystals are commonly observed in the plagioclase of the Bushveld Complex. Among these textures are bent crystals of plagioclase, interpenetration of two adjoining crystals and myrmekite. The last of these apparently only develops under certain conditions and is therefore discussed separately in the next section.

Bent crystals of plagioclase were observed in practically all the thin sections investigated from the Main and Upper Zones. Only in the top 400m or so of the intrusion is this texture rarely observed. The bending of the crystals is indicated by the wedge-shaped and curved polysynthetic twins in the plagioclase (Fig. 45). Fracturing of the crystal at the point of maximum stress can sometimes be seen.

The number of bent plagioclase crystals varies considerably from specimen to specimen and no specific trend could be observed in the sequence.

TABLE VII ZONING IN PLAGIOCLASE FROM THE MAIN AND UPPER ZONES OF THE BUSHVELD COMPLEX

Sample No.	Height in m above MR	Mol. % An core	Mol. % An mantle	Type of Zoning
PB4388	4	75-76	79-82	Reversed
PB4284	35	77	68	Normal
PB4254	44,5	77	75-77	Oscillatory N-R*
PB1101	1005	65	68-65	Oscillatory R-N
PB601	1150	70	65	Normal
G573	1425	65	61	Normal
G577	1515	63	68	Reversed
G583	1740	61	68	Reversed
G584	1880	61	58	Normal
G587A	2065	63	70	Reversed
G435	2580	58	68	Reversed
G515	3200	64	68	Reversed
G365	4625	54	62	Reversed
G351	4637	53	63	Reversed) see
		63	56	Normal) Text
G228	5835	44	48	Reversed
G252	5950	50	42	Normal
G285	6073	43	30	Normal
G208	6140	45	39	Normal
G215	6180	45	40	Normal

*N - Normal
R – Reversed

However, certain horizons do contain more deformed plagioclase crystals than others, especially between 1200 - 1500m and also for short intervals at about 3300 and 3750m above the Merensky Reef.

Interpenetration of two plagioclase crystals (Fig. 46) is a texture fairly commonly observed in the investigated rocks. The term "interpenetrated" was

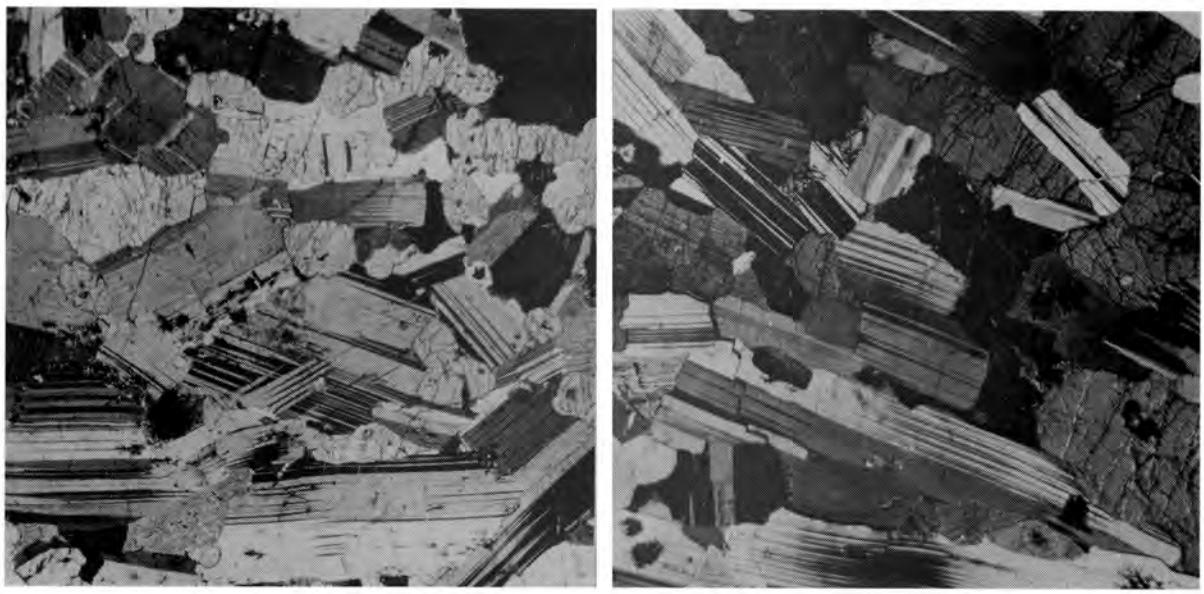

Fig. 45. Numerous bent crystals of plagioclase in plagioclase pyroxene cumulates. G488 (left) and G603 (right). Crossed nicols, x25.

Fig. 46. Interpenetrated crystals of plagioclase. Note the bent, penetrated plagioclase crystal (right), PB2015 (left) PB4076 (right). Crossed nicols, x50

used by Raal (1965, p. 24-25, and Photograph 5) for plagioclase grains which protrude into adjoining grains. He considers the textures to have originated where two settled crystals are in contact with each other in such a way that the corner of the one meets a plane surface of the other. It is suggested by him (p. 55) that partial melting of one feldspar could have taken place at the point of contact if the temperature of the crystals was still close to the temperature of crystallization and if an increase in pressure occurred.

In some cases this texture may be due to crystal settling and adcumulus growth. This is illustrated in Fig. 47A where two cumulus crystals are in contact with each other. Adcumulus overgrowth (solid line) will result in interpenetrating crystals, because each crystal face must compete for space during growth, thus causing an irregular contact between the two (dotted line). Relationships as outlined in Fig. 47B (see also Fig. 47C, points A, B, C, D and E, as well as Fig. 46) cannot be explained in this way. It is highly unlikely that only one crystal will be enlarged by adcumulus growth and not the other. If it is assumed that the solid outlines (Fig. 47B) represent the sizes of the crystals during accumulation then an increase in the pressure would cause a more calcic plagioclase to be stable at the prevailing temperatures. This would result in resolution at the point of stress (the shaded area in Fig. 47B) and in redeposition in the interstices.

A reasonable explanation for the presence of bent plagioclase crystals and interpenetrated relationships between adjoining crystals therefore seems to be compaction owing to an increase in pressure caused by the accumulation of the superincumbent crystal mass.

c) Myrmekite

Myrmekite, by definition an intergrowth of vermicular quartz in plagioclase, is a common constituent of acid plutonic and metamorphic rocks but is extremely rare in calcic plagioclases of mafic intrusions (Barker, 1970, p. 3344). This texture is however present in practically all the gabbroic rocks of the Main Zone of the Bushveld Complex. Its shape and appearance closely resembles that described from granitic rocks and differs only in that it is developed along the grain boundaries of coexisting cumulus plagioclases instead of being associated with alkali feldspars.

The complexity of the myrmekite of the gabbroic rocks in the Main Zone depends largely on the amount of myrmekite present. In all cases, however, it

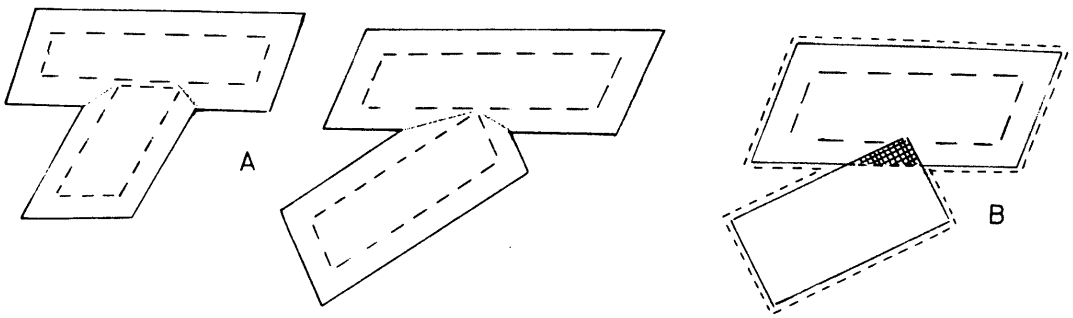

FIG. 47 A AND B. RELATIONS TO ILLUSTRATE DIFFERENCES BETWEEN SIMULTANEOUS CRYSTALLIZATION AND INTERPENETRATION

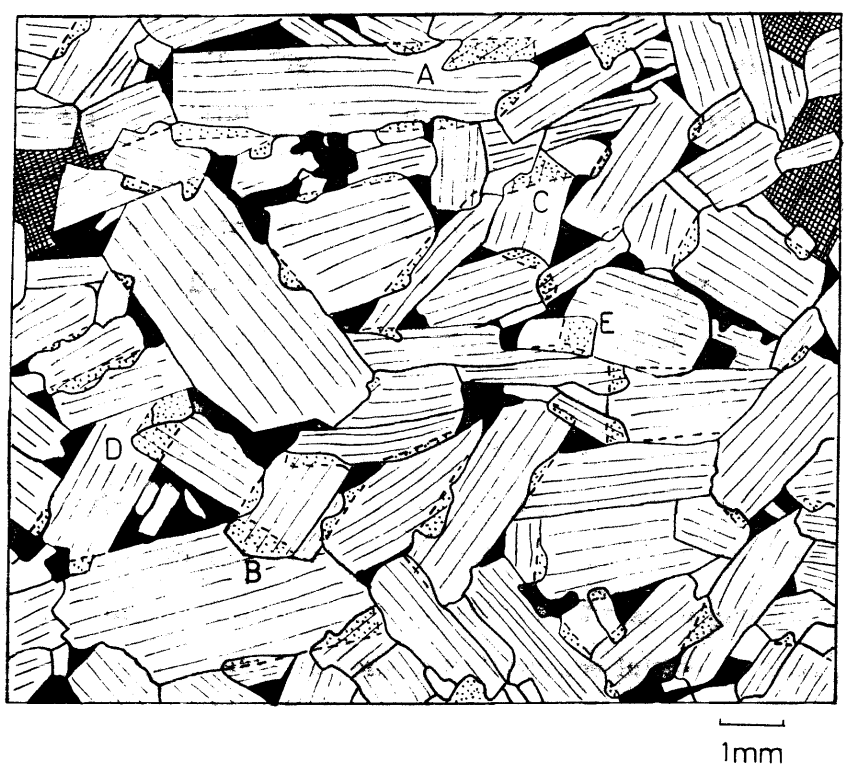

FIG. 47C. MICROGRAPH OF SPECIMEN PB3801 ILLUSTRATING AMOUNT OF INTERPENETRATION (STIPPLED) OF PLAGIOCLASE CRYSTALS. INTERCUMULUS MINERALS: QUARTZ (BLACK), CLINOPYROXENE (HATCHED)

seems to be developed where one plagioclase crystal interpenetrates an adjoining crystal and in many cases, the crystal outline and twinning of the "penetrator" is preserved in the "penetrated", whereas the twinning lamellae of the latter are destroyed (Wager and Brown, Fig. 213, p. 387). The intergrowth seems to advance convexly outwards, and the worms of quartz are orientated perpendicularly to the outer boundary (Fig. 48). At the margin of this intergrowth, the worms tend to be thin and long, and coalesce to form thick, elongated, drop-like inclusions in the central portion. This seems to indicate that the growth has originated at the expense of the penetrated crystal, causing an enrichment of calcium in the penetrator with resultant exsolution of worms of silica.

As the amount of myrmekite increases, the textural relationships also become more complex. This is especially apparent where the two adjoining plagioclases both interpenetrate each other (Fig. 48) and often, relics of the one may be observed in the other. In extreme cases, crystals may be transformed completely to myrmekite (Fig. 49) and often original outlines of the cumulus plagioclase are completely destroyed especially where three or more individuals are involved.

Various theories to explain the myrmekitic textures in granitic rocks have been advanced. Drescher-Kaden (1948, p. 14-104) gives a lengthy discussion of this texture and concludes (p. 102) that it may be due to replacement or corrosion of plagioclase by quartz. However, most authors, who have recently published results of their investigations, favour the theory of unmixing of plagioclase from K-feldspar, because the texture is usually developed between coexisting grains of two alkali-feldspars or between alkali-feldspar and plagioclase. Where this texture is found at grain boundaries of alkali–feldspar and plagioclase, the intergrowth is convex towards the latter. Hubbard (1966, p. 770) explains the texture as being due to exsolution of both the quartz and the plagioclase from the alkali-feldspar, both of which were present as solid solution in the latter at high temperatures. In these cases, the orientation of the more calcic plagioclase of the myrmekite is continuous with that of the primary plagioclase. Shelly (1964, p. 50) on the other hand, believes that the quartz is derived from the interstitial liquid and that the myrmekitic textures resulted from simultaneous crystallization of this quartz and exsolved plagioclase from the alkali-feldspar.

As early as 1909, Schwantke (Barker, 1970, p. 3344), postulated the

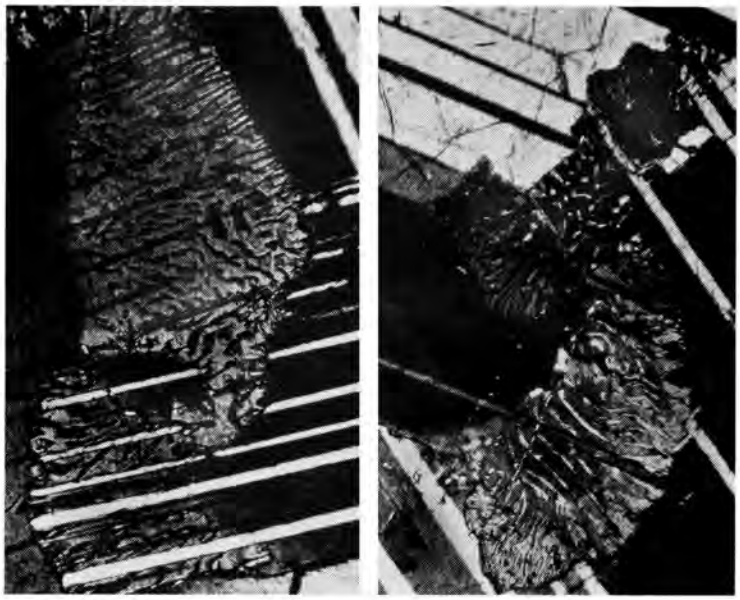

Fig. 48. Complex interpenetration of plagioclase crystals associated with myrmekite. G607. Crossed nicols. x150

Fig. 49. Crystal of plagioclase completely transformed to myrmekite (centre). G609. Crossed nicols, x75

existence of $CaAl_2Si_6O_{16}$ as a compound in solid solution in alkali-feldspar at high temperatures. This has been corroborated by the more recent work of Phillips (1964, p. 58). The amount of $CaAl_2Si_6O_{16}$ exsolved together with albite from the alkali-feldspar would therefore firstly determine the anorthite content of the plagioclase and the amount of quartz in the intergrowth, because these two are apparently controlled by the reaction:

$$CaAl_2Si_6O_{16} \longrightarrow CaAl_2Si_2O_8 + 4SiO_2$$

A close to linear relationship therefore seems to exist between the mole per cent An and the volume per cent quartz in the myrmekite and from volumetric analyses of exsolved quartz, this relationship seems to hold true (Phillips and Ransom, 1968, p. 1412, Barker, 1970, p. 3344).

It is obvious that the above explanation cannot be applied to the gabbroic rocks of the Bushveld Complex, hence Barker's statement (ibid., p. 3339) that "the occurrence of rare calcic myrmekite in mafic rocks remains unexplained", but because of the striking similarities, the mechanism by which these textures originated must be very closely related.

Wager and Brown (1968, p. 387) have pointed out the association of myrmekite with reversed zoning in the Bushveld plagioclases, but as far as could be established during the brief investigation of the textures, reversed zoning can be developed without the presence of myrmekite. During investigation of the thin sections of the sequence, an effort was made to assess the relative abundance of this intergrowth at various levels in the intrusion. The following pattern has emerged from this study:

i) In rocks of Subzone A and the lower half of Subzone B, up to about 2300m above the Merensky Reef, myrmekite is only present in very small amounts. The rocks in this part of the sequence contain fair amounts of intercumulus material (see chapter on modal analyses and Folder IV) and this sequence also includes the orthopyroxene-pigeonite transition zone.

ii) Large quantities of myrmekite are present in the upper half of Subzone B, i.e. where inverted pigeonite proper is developed. Another characteristic of these rocks is the low amount or absence of intercumulus material (Folder IV).

iii) Myrmekite is conspicuously absent in the rocks where primary

cumulus orthopyroxene occurs in Subzone C, but is found in small amounts where ophitic orthopyroxene makes its appearance. Shortly after inverted pigeonite proper appears at the top of this subzone, myrmekite is again abundant, up to the Main Magnetitite Seam.

iv) Above the Main Magnetitite Seam, myrmekite is found in small quantitites, but where symplektitic textures appear about 420m above this seam, myrmekite gradually disappears.

In general, therefore, myrmekite is only developed in abundance where pigeonite proper is present in the rocks and where there is no or very little intercumulus material. Its presence does not seem to be controlled by the composition of the plagioclase, because it is found in plagioclase (An_{63-65}) in the fine-grained norite below the Pyroxenite Marker, whereas plagioclase of similar composition lower down in the sequence, contains hardly any myrmekite.

Other features sometimes observed in the presence of myrmekite are bent crystals of plagioclase. The texture is then often developed where the most deformation of the crystal has taken place, i.e. at the points where the pressure must have been highest to cause bending.

This would seem to indicate that the myrmekite is due to increased load pressure, which would also explain this texture to be associated with interpenetrated plagioclase crystals. On the other hand, rocks which do contain intercumulus material often exhibit interpenetration phenomena, bent plagioclase crystals as well as reversed zoning, but very little or no myrmekite.

From the observed textural relations, it seems as though the development of calcic myrmekite in plagioclase is related to a specific stage in the post-cumulus history of the rock. The abundance of intercumulus material, as well as post-cumulus changes of other mineral phases, for instance the pigeonite-orthopyroxene inversion, seems to affect the change in the feldspar framework.

Deformation of the plagioclase framework owing to load pressure at high temperatures may result in re-solution or recrystallization (interpenetration) at contact points, but owing to equilibration with surrounding intercumulus liquid, the recrystallized or interpenetrated portions will not be more calcic than the rest of the crystal. Deformation at slightly lower temperatures, owing to load pressure and perhaps also owing to a slight shift of the whole cumulus pile during structural rearrangement at the time of the pigeonite-orthopyroxene inversion, and consequently also less intercumulus liquid, may result in non-

equilibration of the recrystallizing plagioclase and cause the calcic myrmekitic intergrowths.

Owing to the interpenetration and bending of the plagioclase crystals, a shortening of the cumulus pile must have taken place, which would suggest the presence of intercumulus liquid prior to and at the time of deformation. Any sodium released during the recrystallization process could have been added to the intercumulus liquid which was continuously pressed out of the pore spaces during compaction.

More detailed information on textural relationships, zoning and the amount of exsolved vermicular quartz is however necessary to determine whether the processes as outlined above may be held responsible for the presence or absence of myrmekite.

d) Orientated inclusions

Long before magnetite appears as a major constituent in rocks of Subzone A of the Upper Zone, the enrichment of iron owing to fractionation is borne out by the presence of tiny rods and "dust" of magnetite in the plagioclase. These inclusions appear at about 2450m above the Merensky Reef and persist up to the base of the fine-grained norite at the top of Subzone B of the Main Zone. They reappear some 250m before the base of the Upper Zone, and continue to be present in plagioclase of Subzones A, B and C, but are practically absent in rocks of Subzone D.

The magnetite inclusions increase southwards in rocks of Subzone B of the Main Zone, so much so that the plagioclase is dark grey to black in hand specimen, forming the well known "black granite" which is quarried at various localities some 40-50km south of the area (Groeneveld, 1970, p. 39).

Where the magnetite needles are well developed, they usually occur in three or more distinct sets in the plagioclase. Their orientation with respect to crystallographic directions of the plagioclase was not determined, as a study of these black gabbroic rocks is at present being undertaken by Mr J. A. van Graan. As far as could be ascertained, none of these sets is orientated parallel to a cleavage direction. Groeneveld (1970, p. 39) mentions that they tend to be orientated parallel to the c-axis of the plagioclase.

Where large amounts of these magnetite rods exist, they are concentrated in the central (cumulus) portion of the plagioclase grains (G409 and G609). This texture is especially well developed in the area under study by Mr J. A.

van Graan, and it is hoped that it will be possible to evaluate the size of the original cumulus crystals, initial porosity prior to adcumulus growth and the post-cumulus enlargement of the plagioclase.

Biotite is often present as tiny flakes embedded in cleavage planes of the plagioclase. This mineral is not considered as an original inclusion, but has probably crystallized at a later stage owing to exsolution of some potassium from the plagioclase at decreasing temperatures.

Fairly common is a mineral which occurs in tiny square or rectangular patches (about 0.02 x 0.03mm) in the central portions of the plagioclase grains. The patches are orientated in such a way that their sides are parallel to cleavage directions of the plagioclase. The refractive index and birefringence of the mineral in these patches seems to be lower than that of the host. The general impression gained is that these inclusions consist of either K-feldspar or quartz.

C. OTHER SILICATES

1. Olivine

Olivine appears in the sequence about 4600m above the Merensky Reef, i.e. at the base of Subzone C of the Upper Zone, although some is also present in rocks at the top of Subzone B (G658, Folder II). Its composition was determined by means of X-ray diffraction, using Co-$K\alpha_1$ radiation and backward reflections in a 114,6mm AEG-Guinier camera as developed by Jagodzinski. The reflection d_{174} and the curve provided by Jambor and Smith (1964, p. 736) were utilized to obtain the molecular percentage of fayalite in the olivine. These values, as well as the composition determined from 2Vx (Tröger, 1959, p. 37) by averaging between 8 and 10 measurements on grain mounts are given in Appendix I. The accuracy of the X-ray determinations is considered by Jambor and Smith (1964, p. 737) to be greater than $\pm$ 1,16 per cent for olivines with composition of Fa_{60} or less, whereas the accuracy decreases slightly for higher Fa values.

In the compositional range Fa_{50}-Fa_{70}, the composition as determined from 2V measurements does not differ much from that derived at from X-ray diffraction, but there are significant differences as the fayalite content increases, the 2V determinations generally giving values of between 8 and 10 mol. per cent Fa too high (Appendix I). Compositions as determined from the X-ray powder data were used in Folder III except the highest Fa value which is based on 2V measurements.

The olivine at the base of Subzone C has a composition of Fa_{49-52} and rises to Fa_{54} in the olivine gabbro associated with the Magnetitite Seam 11. In the olivine diorite below Seam 17, the composition of the olivine is Fa_{69-70}, but rises to Fa_{73} in the rocks directly over and underlying this magnetitite seam. The drop in composition to Fa_{70} directly above Seam 21 is similar, but less, than the reversal in the compositional trend of the plagioclase (Folder III).

Above this magnetitite seam the most iron-rich olivine determined by means of X-ray diffraction has a composition of Fa_{79} 220m below the roof. The composition of olivine, from a sample 175m below the roof was determined as being Fa_{89} by 2V measurements. From reports by Wager and Brown (1968, p. 388) and Molyneux (1970, p. 39) the fayalite content increases to Fa_{100} directly below the roof.

Orthopyroxene and iron-rich olivine frequently coexist as separate cumulus phases especially in rocks of Subzone C of the Upper Zone. In the olivine diorites below Seam 17 in Subzone D, orthopyroxene is however, conspicuously absent, but above this seam it is only present as intercumulus material which is often seen to surround the olivine crystals and a reaction between olivine and the intercumulus liquid to form orthopyroxene cannot be excluded.

Olivine also seems to be a constituent of some of the symplektite which is frequently observed in rocks of the Upper Zone. As several other minerals are involved in these complex intergrowths, they are discussed separately in the section dealing with the postcumulus changes of the rocks.

2. Clinopyroxene

Apart from some observations on the exsolution textures, no work was done on the clinopyroxene of the gabbroic rocks of the Layered Sequence. The reason for this was that determination, by refractive index methods, of the composition of this mineral in the large number of samples which were investigated would have been very time-consuming and the result would probably have been similar to the compositional trend observed for the plagioclase and the orthopyroxene. For the determination of the composition of orthopyroxene and plagioclase, clinopyroxene was also separated. An investigation of the compositional variations of this mineral is intended at a later stage. Recently, Atkins (1969, p. 239) published several analyses of Ca-rich pyroxene from the Bushveld and determined, among other things, their trend of crystallization (ibid., Fig. 3).

Of interest are the observed exsolution textures in the augite. Hess and Poldervaart (1951, p. 481) pointed out that exsolution-lamellae of orthorhombic pyroxene in monoclinic pyroxene or vice versa are parallel to the (100) plane, whereas monoclinic pyroxene exsolves parallel to (001) in another monoclinic pyroxene. Hypersthene therefore exsolves parallel to the (100) plane and pigeonite parallel to the (001) plane of augite. Brown, (1957, p. 527) states that it is to be expected that the type of pyroxene exsolved from the augite would be the same as the coexisting cumulus pyroxene. Augite in the majority of rocks investigated, however, contains two sets of exsolution-lamellae irrespective of whether the coexisting cumulus phase is hypersthene or inverted pigeonite.

In Subzone A and B of the Main Zone, exsolution-lamellae parallel to the (100) plane of augite are the most abundant, and although lamellae parallel to (001) are present and increase upwards in the sequence, they remain subordinate. The (100) lamellae are usually thin, well developed and traverse the whole grain, whereas the (001) lamellae are short and usually thicker. At the base of Subzone C only (100) lamellae are present, but towards the top (001) lamellae are also developed.

In Subzone A of the Upper Zone, thin, well developed (100) lamellae still predominate over the short and thick (001) lamellae, although the latter are more numerous than at the top of the Main Zone. A reversal in the abundance of the two types of exsolution-lamellae takes place in Subzone B of the Upper Zone. At the base of this subzone the two types seem to be developed in equal amounts, but the (001) lamellae increase and predominate towards the top. In Subzone C only a few (100) lamellae are present at the base but are absent at the top. The (001) lamellae are now thin and traverse the whole grain whereas the few (100) lamellae are short and usually slightly thicker. The augite in the predominantly olivine-bearing rocks of Subzone D contains hardly any exsolved lamellae of clinopyroxene, but where they are developed, they are extremely thin and orientated parallel to the (001) plane of the host.

The observed exsolution textures are, for the greater part of the succession not difficult to explain, but the presence of two sets of exsolution-lamellae in Subzone A of the Main Zone where the coexisting Ca-poor pyroxene is primary hypersthene, presents a problem. In these rocks only (100) exsolution-lamellae are expected as this is the direction parallel to which the orthorhombic substance exsolves in the augite. The presence of a few (001) exsolution-lamellae

would seem to indicate that, perhaps at high temperatures, some of the orthopyroxene was exsolved parallel to that direction.

Higher in the sequence, i.e. in the orthopyroxene-pigeonite transition zone, the coexistence of two sets of lamellae can be explained in conjunction with the hypothesis concerning the coexistence of inverted pigeonite and primary hypersthene. As postulated, when the magma entered the stability field of three pyroxenes (Fig. 44a point p) pigeonite would crystallize and consequently is also the phase which exsolved parallel to the (001) plane in coexisting cumulus augite. Slight cooling of the crystallizing magma at constant Fe/Mg ratio would result in hypersthene becoming the stable Ca-poor pyroxene and any further exsolution in augite would be parallel to the (100) plane. The presence of exsolution-lamellae parallel to (001) and (100) of augite in certain rocks of the Skaergaard Intrusion led Brown (1957, p. 528) to suggest that both orthopyroxene and pigeonite could have been in equilibrium with the augite during crystallization of these rocks.

Where inverted pigeonite is the only Ca-poor phase in the rocks, two sets of exsolution-lamellae are usually developed in the augite, i.e. at the top of Subzones B and C of the Main Zone as well as in Subzones A and B of the Upper Zone. In the augite of these rocks, pigeonite was exsolved parallel to the (001) plane above the inversion temperature and hypersthene parallel to the (100) plane below the inversion temperature. As the temperature interval between crystallization of pigeonite and inversion to hypersthene increased, more and more of the monoclinic phase would be exsolved from the augite before the inversion, to such an extent that in the lower half of Subzone B of the Upper Zone, the two exsolution sets are equally abundant, but at higher levels the (100) exsolution-lamellae decrease and are absent at the top of Subzone C. Where orthopyroxene makes way for olivine in Subzone D of the Upper Zone the augite contains hardly any exsolution-lamellae and those which are present are extremely thin and orientated parallel to the (001) plane.

3. Biotite

During the separation of the minerals from specimens of the Main and Upper Zones, it was possible to separate relatively pure biotite where this mineral was present in fairly large quantities. One of these specimens is from Subzone A of the Main Zone and the others are from the Upper Zone. X-ray powder diagrams were obtained from these on an AEG-Guinier camera with

Co-Kα_1 radiation. The purpose of this study was to determine whether there are any variations in the value of the 060 reflection, which, according to Wones (1963, p. 1305) shows the greatest shift with changes in the Fe/(Fe + Mg) ratio in the annite-phlogopite solid solution series. The results are given in Table VIII and are diagrammatically presented in Fig. 50.

Wones (1963, p. 1307) has shown that there is a systematic increase in d_{060} with increase of the Fe/(Fe + Mg) ratio for a given oxygen fugacity and a systematic decrease in d_{060} at constant Fe/(Fe + Mg) as the oxygen fugacity increases. From Fig. 50 it may be seen that the d_{060} of biotite from the specimen of the Main Zone is lower than all those of the Upper Zone, which may be due to an increase in the Fe/(Fe + Mg) ratio. The d_{060} values of biotite from the Upper Zone fluctuate considerably even over short intervals (G620, G621, G310, Table VIII), so much so that the difference in Fe/(Fe + Mg) between samples G620 and G310 at any given constant oxygen fugacity (ibid., Fig. 3) is as much as 0,3. Differences in the Fe/(Fe + Mg) ratios of the other ferromagnesian silicates never show such variations over short distances as this and it follows that different oxygen fugacities may be held responsible for some of the observed fluctuations.

TABLE VIII d_{060} VALUES OF BIOTITE FROM ELEVEN SAMPLES OF THE MAIN AND UPPER ZONES

Sample No.	Height in m above M.R.	$2\theta(\pm 0,025)$ $CoK\alpha_1$	d_{060} (Å)
PB2015	720	70,94	1,5414
G400	4083	70,53	1,5490
G510	4110	70,50	1,5498
G568	4275	70,62	1,5479
G617	4804	70,43	1,5509
G620	4828	70,38	1,5521
G621	4849	70,59	1,5482
G310	4865	70,77	1,5448
G253	5960	70,63	1,5479
G368	5990	70,47	1,5505
G285	6075	70,31	1,5536

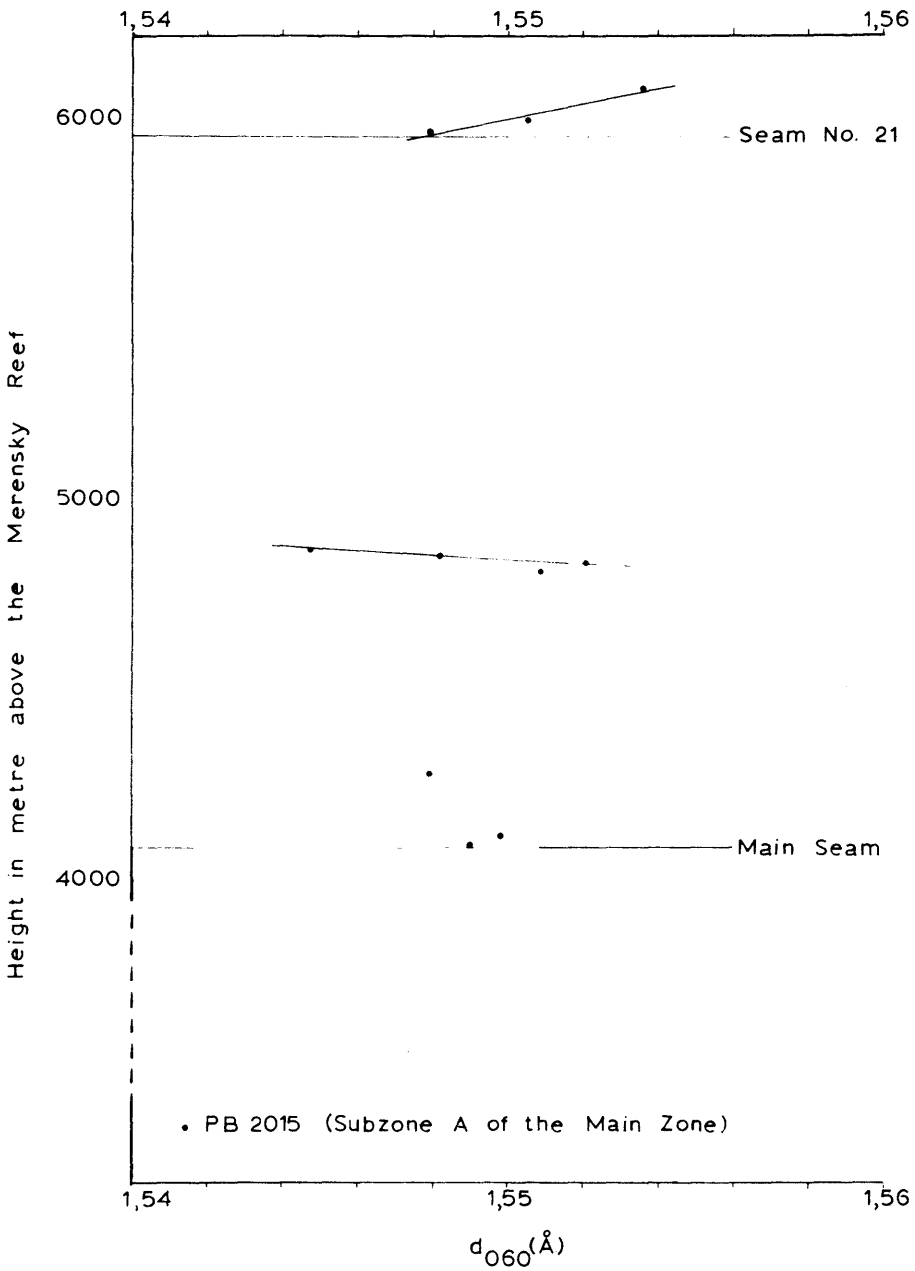

FIG. 50. VARIATION OF d_{060} OF BIOTITE IN THE UPPER ZONE

Seeing that biotite in all these rocks is intercumulus and in some rocks also a product of reaction (see description of symplektite in the section on postcumulus changes) it follows, from the fluctuating d_{060} values, that the oxygen fugacity in the intercumulus liquid changed considerably from one level in the intrusion to the next during crystallization. This may in part be due to changes in load pressure on the water-enriched intercumulus liquid, which is to some extent indicated by bent plagioclase crystals, reversed zoning of this mineral and the presence of various types of pegmatoids.

D. APATITE

1. Introduction

Apatite is an important constituent of the late differentiates in many layered intrusions throughout the world (Wager and Brown, 1968) and is known to be present in the rocks of the Upper Zone of the Bushveld Complex from many reports (Daly, 1928, p. 738; Boshoff, 1942, p. 28; Wager and Brown, 1968, p. 380; Willemse, 1969a, p. 13; Grobler and Whitfield, 1970, p. 208). Very little is, however, known about apatite in gabbroic rocks, and although various analyses exist (Taborszky, 1962, p. 368-369; Cruft, 1966, p. 382-383) the behaviour of this mineral with differentiation in a layered intrusion has not yet been studied.

It is commonly known that magmatic apatite may contain F, OH and Cl in various amounts, the relative abundances of which may give some indication of the environment of crystallization (Taborszky, 1962, p. 373-375). Apatite can also accommodate a large variety of trace elements which are also to some extent indicative of the magma from which the apatite has crystallized (ibid., p. 376; Cruft, 1966, p. 384). If this is borne in mind, as well as the fact that the rocks in layered intrusions are characterized by a gradual change in composition from bottom to top, small changes in abundance of certain elements in apatite from various heights in layered intrusions are to be expected.

Consequently, considerable time was spent on separating sufficient amounts of apatite from rocks of Subzone D of the Upper Zone where it occurs as cumulus crystals, generally in abundance of more than 3 per cent by volume (Folder IV). These samples were submitted to Dr P. J. Fourie of the Atomic Energy Board for analyses of the main and trace elements, but the results are unfortunately not yet available.

2. Microscopic investigation

a) General

Cumulus apatite is present as small idiomorphic crystals throughout the olivine-bearing rocks of Subzone D, and although mostly concentrated along grain boundaries between the silicates, it is also common as inclusions in the silicates and in magnetite (Fig. 51). Apatite occurring as inclusions is usually small, whereas that between the grain boundaries is larger. From this it is reasonable to assume that it started to crystallize early, and judging from the intercumulus nature of some of the grains, it probably crystallized until the final stages of consolidation. The small crystals were therefore trapped in the faster growing silicates, whereas others were pushed out of the way. For this reason, the larger apatite grains are often found to be intimately associated with the products of late crystallization (intercumulus material) such as titanomagnetite and biotite. For the modal distribution of apatite see the chapter on Modal Analyses, Folder IV and Appendix I.

b) Grain size

The size of the apatite crystals depends to a certain extent on the abundance of this mineral in the rock. For instance, in G200 and G201, where the apatite content is only about 0,5 per cent, the average dimensions of the crystals are 0,18 x 0,05mm, whereas in G253 where the apatite constitutes 8,5 per cent by volume of the rock, the average dimensions are 0,75 x 0,14mm. The largest apatite crystals were however found in a pegmatoidal rock (DDH2-248) some 30m below the Magnetitite Seam 21 in the bore-hole on Doornpoort 171 JS. Although crystals measuring up to 1,42 x 0,25mm and 1,25 x 0,55mm are present, the apatite content of this rock does not exceed 4 per cent.

c) Orientated inclusions

Many of the apatite crystals in the separated samples contain small rod-like inclusions usually orientated parallel to the c-axis of the apatite (Fig. 52). These inclusions consist either of biotite or of a green pleochroic mineral. In a few grains small specks of ore, probably magnetite, are also present as inclusions. Taborszky (1962, p. 365) mentions hornblende as inclusions in apatite from the Odenwald and it is possible that the green pleochroic mineral in the apatite of the Bushveld Complex is also hornblende. These inclusions are however, difficult to explain for the following reasons:

i) Biotite is always present in these rocks as intercumulus material and its presence in the centre of the apatite crystals, which are considered to be products of early crystallization, is therefore problematic.

ii) Hornblende is a primary intercumulus constituent only in rocks of the top 100m of the intrusion.

Some of the apatite crystals contain biotite and the green pleochroic mineral in one and the same inclusion and for this reason the latter mineral may also be considered as an alteration product of the biotite, possibly chlorite.

The biotite in the apatite is elongated parallel to its c-axis and the impression gained is that there seems to be an epitaxial relationship between these two minerals. From microscopic observations (Fig. 52) it seems as though the (010) and (110) planes of the biotite coincide with the prism faces of apatite. If these are the lattice planes in the two minerals on which the orientated overgrowth has taken place, then it follows that a_o of apatite must correspond to $2a_o$ of biotite and the c_o of apatite, or a multiple thereof, to c_o of biotite.

Deer et al. (1962, v. 3 p. 55 and v. 5 p. 324) give the following cell parameters for biotite and fluorapatite.

Biotite:	$a_o = 5,3$ Å	Apatite:	$a_o = 9,35$ Å
	$b_o = 9,2$ Å		$c_o = 6,87$ Å
	$c_o = 20,2$ Å		

There is a good correlation between $2a_o$ of biotite and a_o of fluorapatite, as well as between c_o of biotite and $3c_o$ of fluorapatite (20,61 Å). The differences between the cell parameters fall well within the 10-15 per cent permissible tolerance (Neuhaus, 1951, p. 156). Although there is a better correlation between b_o of biotite and a_o of fluorapatite, such an overgrowth would necessitate a morphological (100) plane of biotite, conditions under which the prism faces of biotite would not be parallel to those of apatite and would therefore not agree with the observed relationships (Fig. 52, bottom row).

Neuhaus (1951) gives a detailed review of researches on apitaxy whereas Von Vultée (1951) lists numerous examples of natural occurences of orientated intergrowths recorded in the literature prior to 1951. From Von Vultee's compilation, not much seems to be known about orientated inclusions in apatite.

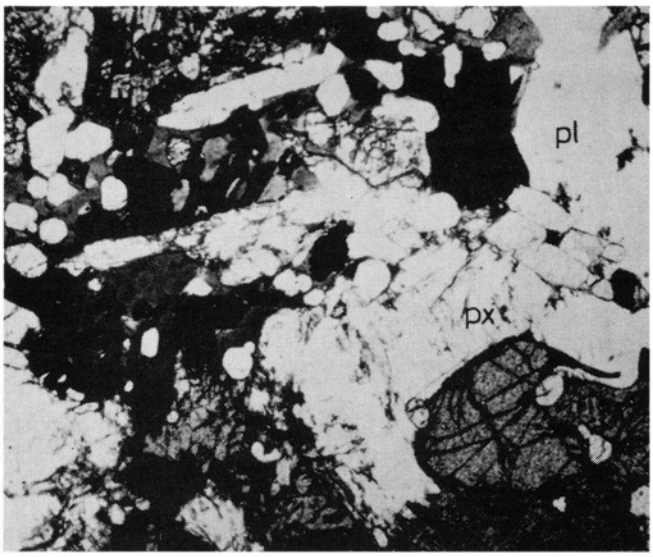

Fig. 51 Apatite-rich olivine diorite directly overlying Magnetitite Seam 21. Note small inclusions in olivine (bottom right) and larger crystals between pyroxene (px) and plagioclase (pl). G253, Duikerkrans 173 JS. x50.

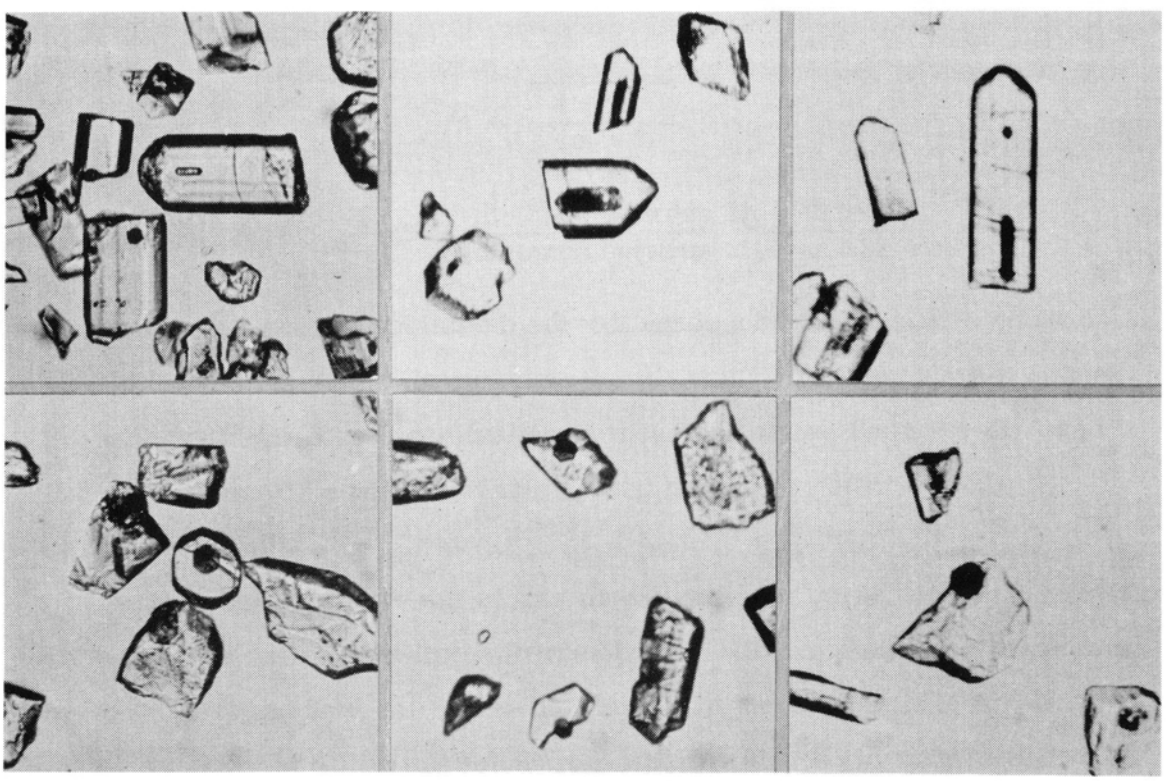

Fig. 52 Inclusions orientated parallel to the c-axis of apatite (top row). The inclusions have hexagonal outlines when viewed in (0001) cleavage fragments (bottom row). Apatite concentrates from various specimens, x100.

He mentions (ibid., p. 337) monazite and opaque ore parallel to the c-axis of apatite and ilmenite parallel as well as perpendicular to the c-axis of apatite. Orientated intergrowth of muscovite (host) and apatite is however recorded (p. 344) but none of the cited directions coincide with the observed ones.

3. Determinative methods

a) X-ray investigations

i) Method

X-ray powder data were obtained by using an AEG Guinier camera developed by Jagodzinski, with Cu-$K\alpha_1$ radiation and silicon as internal standard. The minerals were indexed with the aid of the Powder Data File, card No. 15-876. Cell dimensions c_o and a_o were calculated by using the reflections 00.4 and 41.0 respectively. The observed $\sin^2\theta$ values were compared with the $\sin^2\theta$ values which were calculated by using the determined cell parameters. Seeing that the differences are less than 0,00015, an accuracy of $\pm$ 0,003Å for the cell dimensions is indicated. The c/a ratio was also calculated after the method of Brasseur as modified by Förtsch (1970, p. 224), namely,

$$c/a = \sqrt{\frac{4 + 2m}{4m + 7}}$$

$$\text{where } m = \frac{\text{distance between 41.0 and 00.4}}{\text{distance between 21.3 and 32.1}}$$

The value of m is obtained by direct reading of the distances between the pairs of lines on the film. In most cases, the values obtained by this method differed only in the fourth decimal from those calculated from the 41.0 and 00.4 reflections. The results of this investigation are given in Table IX.

ii) Results

The most striking result of this investigation is borne out by the variation of the a_o value with height in the intrusion (Fig. 53). Apatite from the lowest horizon (G271) has an a_o of 9,388 Å. This value increases gradually to 9,417 Å, 70m below the roof of the intrusion from where it drops abruptly to 9,374 Å directly below the roof (G200).

Comparison of these results (Table IX) with the unit cell dimensions of the end-members of apatite, reproduced here from Deer et al. (1962, v. 5, p. 324) leads to the following conclusions:

TABLE IX PHYSICAL PROPERTIES OF APATITE FROM THE UPPER ZONE OF THE BUSHVELD COMPLEX

Sample No.	G271	G264	G257	G253	G368	G285	G208	G216	G215	G214	G201	G200
Height in m above M. R.	5350	5650	5735	5960	5990	6075	6140	6165	6180	6200	6207	6209
n_o (±0,002)	1,638	1,637	1,637	1,638	1,639	1,639	1,640	1,639	1,638	-	1,638	1,638
n_E (±0,002)	1,634	1,633	1,633	1,635	1,636	1,635	1,636	1,635	1,634	-	1,634	1,634
$(n_o - n_E)$	0,004	0,004	0,004	0,003	0,003	0,004	0,004	0,004	0,004	-	0,004	0,004
D (±0,01)	3,23	3,22	3,23	3,23	3,22	-	3,24	3,26	3,25	-	-	-
a_o (Å) (±0,003)	9,388	9,394	9,396	9,406	9,405	9,405	9,417	9,408	9,400	9,378	9,379	9,374
c_o (Å) (±0,003)	6,873	6,872	6,885	6,873	6,882	6,878	6,881	6,870	6,872	6,885	6,881	6,881
c/a calc.	0,732	0,732	0,733	0,731	0,732	0,731	0,731	0,731	0,731	0,734	0,734	0,734
c/a meas.	0,732	0,732	0,733	0,731	0,732	0,732	0,731	0,731	0,732	0,734	0,734	0,734

Unit cell dimensions of end-members of apatite

	a(Å)	c(Å)	c/a
Fluorapatite	9, 35	6, 87	0, 735
Chlorapatite	9, 61	6, 76	0, 704
Hydroxyapatite	9, 41	6, 87	0, 731

The a_o value of the first cumulus apatite is 9, 388 Å and is intermediate between that of fluorapatite and hydroxyapatite, whereas the c_o value corresponds closely to these two. This would seem to indicate that this apatite contains appreciable amounts of F and OH. The increase in a_o to 9, 417 Å points to a decrease in the F and an increase in the OH content of the apatite and specimen G208 therefore seems to be a relatively pure hydroxyapatite. The sudden drop in a_o from 9, 417 Å to 9, 374 Å in the top 70m of the intrusion is probably due to a sharp increase in the F component of the apatite.

The calculated unit cell dimensions would not favour any large amounts of Cl in the apatite, as these values differ considerably from those of chlorapatite. The ionic radius of Cl is 36 per cent and that of OH 5 per cent larger than that of F. An isomorphous series therefore exists between fluorapatite and hydroxyapatite, and these apatites are only able to accommodate limited amounts of Cl in their structure (Taborszky, 1962, p. 384). Taborszky (1962, p. 308) who studied apatites from the Odenwald, found that they are essentially fluorapatites with fair amounts of OH but very little Cl. He also found that the F/OH ratio in apatite is high in acid rocks and decreases in mafic rocks (p. 373 and 375). From this it is to be expected that the F/OH ratio should gradually increase with differentiation, but unit cell dimensions of apatite from the Upper Zone of the Bushveld Complex point to a considerable decrease in this ratio prior to an increase in the top 70m of the intrusion.

Stormer and Carmichael (1971, p. 130) came to the conclusion that in apatite and phlogopite (biotite) which are in exchange equilibrium with fluorine and hydroxyl at magmatic temperatures, there is a tendency for the F to occupy approximately 75 per cent of the halogen sites in the former and between 60 and 75 per cent in the latter. They point out that there was either a shortage of fluor, or late stage exchange at low temperatures where natural assemblages do

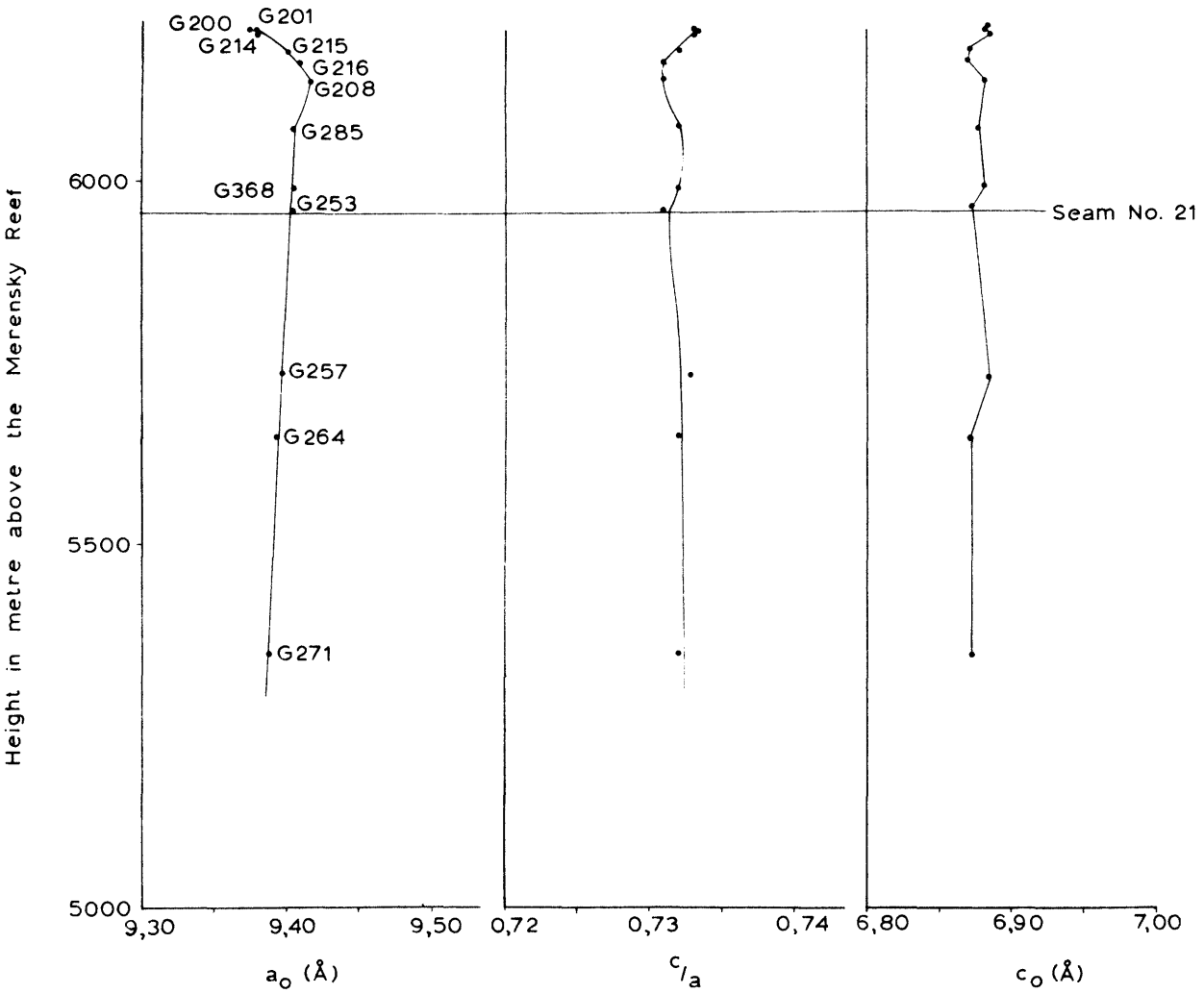

FIG. 53. VARIATION OF UNIT CELL PARAMETERS OF CUMULUS APATITE IN SUBZONE D OF THE UPPER ZONE

not show this relationship. Their results indicate that F has an affinity for apatite and that a F-rich apatite will crystallize from a magma if sufficient F is present.

It may therefore be concluded that at the beginning of crystallization of apatite, fluorine was present in fair amounts in the magma but that due to crystallization of the apatite its concentration in the magma decreased gradually. This probably resulted in more and more of the hydroxyl being incorporated in the apatite structure. The reversal in the top 70m of the intrusion is not ascribed to an increase in the fluorine content of the magma but to a decrease in its phosphorus content which resulted in a decrease in the amount of apatite in these rocks (Folder IV). Larger amounts of fluorine were therefore available for the smaller amounts of apatite which crystallized at the top, thus causing this reversal.

b) Refractive index and density

Routine refractive index determinations were made by means of the immersion method, the results of which are given in Table IX. It is evident that no conclusions can be drawn regarding the relative abundance of the F, OH and Cl content of the apatite, because the method used only allows for an accuracy of $\pm$ 0,002. These determinations do, however, show an increase in the refractive index with an increase in the a_o value.

The few density determinations, made according to the method outlined by Jahns (1939, p. 119-120), also show an increase with higher a_o values. Refractive index and density of the apatite therefore seem to increase with higher hydroxyl content.

4. Petrogenesis

Apatite is present in minute amounts as intercumulus material in many of the rocks of the Main and Upper Zones (Folder IV; Appendix I). It appears abruptly as a cumulus phase at the base of Subzone D in the Upper Zone and generally constitutes between 4 and 6 per cent by volume of the rocks. This would seem to indicate that most of the phosphorus remained in the magma during crystallization of the greater part of the Layered Sequence. Enrichment of this element in the remaining magma would be enhanced by adcumulus growth. Any phosphorus in rocks below Subzone D therefore seems to be present in intercumulus apatite and since cumulus minerals such as plagioclase, olivine and pyroxene are essentially devoid of this element, Wager (1963, p. 6)

concluded that the amount of P_2O_5 in analysed cumulates is an indication of the amount of trapped liquid. Henderson (1968, p. 907) has, however, shown that, although of a low order, phosphorus enters cumulus minerals and may, in some instances, comprise most of the phosphorus in certain adcumulates.

Wager (1960, p. 378-381) calculated the amount of P_2O_5 in successive residual liquids of the Skaergaard Intrusion and concluded that cumulus apatite began to crystallize when the concentration of phosphorus in the magma was 7500ppm (1,75 per cent P_2O_5) (Wager and Brown, 1968, p. 201). Peck et al. (1966, p. 653) also found that P_2O_5 is concentrated in the differentiated liquids (oozes) confined to the interstices of crystallizing tholeiitic basalt in the Alae Lava lake of Hawaii and it was even possible for them to plot this increase in P_2O_5 in the liquids as a function of the temperature of formation of the oozes (ibid., Fig. 11, p. 652). They found that apatite appears as tiny needles in the interstitial glas at 1000°C, and extrapolation of their Fig. 11 reveals that this necessitates a P_2O_5 concentration of about 1,8 per cent (7700ppm P), a value which agrees closely with that determined by Wager and Brown (1968, p. 201). From this it may be concluded that apatite started to crystallize when the phosphorus content of the Bushveld magma was in the vicinity of 7500-7700ppm.

The association of cumulus apatite with olivine and its absence in the olivine-free rocks associated with Magnetitite Seams 17 to 21 (Folder IV; Appendix I) is difficult to explain, but is probably governed by conditions in the magma chamber leading to the precipitation of magnetitite seams. If it is assumed, as proposed by Roeder and Osborn (1966, p. 452-455), that fractionation of magma during the crystallization of the Fe-rich olivines took place at low oxygen pressures i. e. in a closed system where the oxygen content of the crystallizing mixture remains constant, then the associated cumulus apatite would seem to favour similar conditions for crystallization. A constant pO_2 during fractional crystallization causes a change in the oxygen content of the mixture and an increase in the oxygen content of the condensed phases (ibid., p. 454; Hamilton and Anderson, 1967, p. 464). If the oxygen pressure is sufficiently high, it favours crystallization of magnetite. The presence of cumulus magnetite in the apatite-bearing olivine diorites of the Upper Zones would therefore indicate fairly high, constant pO_2 conditions. A slight rise in the pO_2 would probably augment crystallization of magnetite to form magnetitite seams and cessation of crystallization of olivine, conditions under which apatite also did not crystallize.

During the formation of the magnetitite seams of Subzone D, the phosphorus content of the magma therefore increased with the result that when conditions returned to "normal" (i. e. slightly lower oxygen pressure) the crystallizing rocks were enriched in apatite. The highest percentage of apatite (8, 5 per cent by volume) is in rocks directly overlying Magnetitite Seam 21.

Simultaneous crystallization of olivine and magnetite, as indicated in Seam 21, would point to an extreme iron enrichment in the magma, so much so that only a slight increase in oxygen pressure was sufficient to cause abundant crystallization of magnetite but not sufficient to stop crystallization of olivine. The olivine-apatite magnetitites in the Villa Nora area, which contain up to 30 per cent apatite (Grobler and Whitfield, 1970, p. 219), on the other hand, would indicate a simultaneous oversaturation of phosphorus in this locality, so much so that crystallization of large quantities of magnetite did not influence the crystallization of the apatite. Grobler and Whitfield (1970, p. 225) are however of the opinion that these lenticular magnetitite bodies could possibly have formed by a process of residual liquid accumulation and immiscible liquid segregation. This immiscible liquid was then injected concordantly into the host rocks. The available evidence, as cited by these authors indicates that the conditions of formation of these bodies were different from those of the normal apatite-bearing rocks in the area mapped, as well as in other areas of the complex.

E. THE SULPHIDES IN THE UPPER ZONE

1. Introduction

The various sulphides which are present in the Layered Sequence of the Bushveld Complex have already been described in detail by Liebenberg (1970, p. 115-141). Therefore, the purpose of this study is not to describe the various sulphide minerals again, but rather to describe their occurrence in the various horizons present in the area examined. Three mineralized horizons were described by Liebenberg in the sequence dealt with in this investigation: the mineralized anorthosite below the Main Seam, that below the uppermost magnetitite seam, and a mineralized magnetite gabbro some distance above the Main Magnetite Seam in the vicinity of Magnet Heights. This last horizon was not found to be mineralized in the area investigated, although it must be mentioned that outcrops at this particular horizon are not very good. Two additional horizons were found to be mineralized in this area, namely, a mineralized

anorthosite below Lower Magnetitite Seam 2, and concentrations of sulphides in the uppermost magnetitite seam.

In Table X the volumetric composition of the sulphide phase in the various rock groups and mineralized horizons are presented. The values given by Liebenberg (1970, p. 163) for the mineralized horizons of the Upper Zone, have been included for comparison. The following methods were used to attain the values in this table:

a) Conventional point count analyses were made on various polished sections of the mineralized horizons with the aid of a Swift Automatic point counter. (1, 3, 11 and 12, Table X).

b) The ordinary gabbroic rocks usually contain 0,5 vol. per cent or less sulphides. To obtain reasonable values for the various sulphide phases, the cross-hair in the ocular was replaced by a glass disc with a grid engraved on it. The polished sections were placed on a mechanical stage and the sulphide phases at the intersections of the grid lines were counted. Because of the low sulphide content of these rocks, the values given in columns 6, 7, 8, 9, 13 and 14 of Table X do not represent specific horizons in the intrusion, but the average sulphide content of several specimens from characteristic rock units.

2. Variation of the minerals in the sulphide phase

In his description of the sulphides of the Bushveld Complex, Liebenberg (1970, p. 141-147) found certain variations in the mineral composition of the sulphide phase with height in the intrusion. He found (p. 146) that pyrrhotite increases with height in the Upper Zone and attains a maximum value in the mineralized anorthosite below the Magnetitite Seam 21. Chalcopyrite attains its maximum value in the ordinary magnetite-bearing gabbroic rocks but makes way for pyrrhotite in the olivine-bearing rocks. Pentlandite decreases gradually with height in the intrusion whereas pyrite is the most abundant sulphide in the uppermost differentiates (diorites) of the Complex.

The results of this investigation generally confirm Liebenberg's findings but as a larger number of samples from this sequence has been examined, more information concerning the sulphide phase has been obtained.

In the magnetite-bearing anorthosites and gabbros, pyrrhotite increases from 31,2 per cent (Table X; Fig. 54a) in the mineralized anorthosite below Lower Magnetitite Seam 2 to 75,3 per cent (7, Table X) in magnetite gabbros of Subzone C. In all the olivine-bearing rocks above the magnetite gabbros of

TABLE X VOLUMETRIC COMPOSITION OF THE SULPHIDE PHASE IN VARIOUS HORIZONS OF THE UPPER ZONE

	1	2*	3	4*	5*	6	7	8	9	10*	11	12	13	14
Pyrrhotite	31,2	51,0	55,6	57,3	55,1	54,7	75,3	96,7	95,4	85,6	81,6	95,1	95,7	15,4
Pentlandite	5,9	5,4	5,5	4,8	5,1	1,8	1,2	0,5	0,4	7,6	-	0,3	0,2	tr.
Chalcopyrite	55,0	34,9	35,6	35,7	38,2	37,4	22,6	2,7	4,0	6,4	6,6	2,6	3,1	2,6
Pyrite	7,9	8,3	3,3	1,6	0,8	3,1	0,9	-	tr.	-	2,0	1,9	0,7	81,5
Sphalerite	tr,	0,2	tr.	0,2	0,4	-	tr.	tr.	0,2	0,4	9,6	0,1	0,25	0,5
Cubanite	-	-	-	-	-	3,0	-	0,1	-	-	-	-	-	-
Mackinawite	-	0,1	-	-	0,2	tr.	-	tr.	-	-	-	-	-	-
Galena	-	-	-	-	-	-	-	-	tr.	-	0,2	-	0,05	-
Gersdorffite	-	-	-	-	0,3	-	-	-	-	-	-	-	-	-
No. of points counted	4874	-	2155	-	-	3561	3113	4818	4276	-	4932	2224	6259	1976
No. of sections averaged	4	-	2	-	-	6	4	4	6	-	3	4	5	5

*Values taken from Liebenberg 1970, p. 193.

For sample localities see Table XI.

Subzone C, pyrrhotite constitutes more than 95 per cent of the minerals in the suphide phase. The mineralized anorthosite below Magnetitite Seam 21 however, contains less pyrrhotite (No. 11, Table X). In the diorites at the top of the intrusion, pyrrhotite decreases sharply to 15, 4 per cent of the sulphides (No. 14, Table X).

Chalcopyrite attains its maximum value of 55, 0 per cent in the mineralized anorthosite below Lower Seam 2. It gradually decreases upwards in the intrusion to 22, 6 per cent in the ordinary gabbroic rocks of Subzone C. Above this horizon, the chalcopyrite drops to less than 4 per cent and remains fairly constant in all the olivine-bearing rocks. There is a slight increase in this mineral in the mineralized anorthosite below Magnetitite Seam 21.

Pentlandite decreases gradually with height, irrespective of whether olivine is present or not. Of interest is the high pentlandite content recorded by Liebenberg in the mineralized anorthosite below the uppermost magnetitite seam. An increase in the pentlandite content at this horizon is to be expected if the general reversal of the trend of the other sulphides at this horizon is considered (Table X). The sections investigated in this study did not contain any pentlandite in measurable quantities, and one section in particular was found to contain 36 per cent sphalerite (DDH2-243). No explanation for this anomaly can be offered.

Pyrite is present in small quantities in the gabbroic rocks below the olivine-bearing rocks of Subzone D. It is conspicuously absent in the olivine-bearing rocks below the uppermost magnetitite seam, but appears again in this seam and in the overlying olivine-bearing rocks. It is the most common sulphide in the topmost differentiates (diorites) of the intrusion.

The association of pyrite and cubanite in the magnetite gabbros of Subzone B (column 6, Table X) is anomalous. Pyrite is present in two of the six sections from this subzone (G569 and G510), whereas cubanite was found to be developed in four of these six sections (G351, G422, G510 and G652). Only in one of these sections does cubanite occur together with pyrite. The textural relations suggest that the cubanite is a primary mineral of the early separated sulphide phase, whereas pyrite, seems to have replaced pyrrhotite at a very late stage. This association will be discussed in more detail further on.

In Table XI the proportions of the major elements in the sulphide phase have been calculated from the values given in Table X, and by using densities

TABLE XI WEIGHT PER CENT OF THE MAJOR ELEMENTS IN THE SULPHIDE PHASE OF THE VARIOUS HORIZONS. (Calculated from the values given in Table X).

Element	1	2	3	4	5	6	7	8	9	10	11	12	13	14
Fe	41,6	47,5	48,1	48,3	47,5	48,1	53,6	59,5	59,0	56,0	53,1	58,4	59,2	48,0
Ni	2,2	2,0	2,0	1,8	1,9	0,7	0,4	0,2	0,1	2,7	–	0,1	0,1	–
Cu	18,0	11,3	11,6	11,6	12,5	13,0	7,3	0,7	1,3	2,0	2,1	0,7	1,0	0,7
Zn	–	0,1	–	0,1	0,3	–	–	–	0,1	0,2	5,7	–	0,3	0,1
S	38,2	39,1	38,3	38,2	37,8	38,2	38,7	39,5	39,5	39,1	39,1	39,8	39,6	51,0

1. Mineralized anorthosite below Lower Magnetitite Seam 2, Zwartkop 142 JS.
2. Mineralized anorthosite below the Main Magnetitite Seam, Zwartkop 142 JS (Liebenberg, 1970, p. 193).
3. Mineralized anorthosite below the Main Magnetitite Seam, Zwartkop 142 JS.
4. Mineralized anorthosite below the Main Magnetitite Seam, Magnet Heights (Liebenberg, 1970, p. 193).
5. Mineralized anorthosite 70m above the Main Magnetitite Seam, Magnet Heights (Liebenberg, 1970, p. 193).
6. Sulphides in the magnetite gabbros of Subzone B. Luipershoek 140 JS and Mapochsgronde 500 JS.
7. Sulphides in the magnetite gabbros of Subzone C. Luipershoek 140 JS.
8. Sulphides in olivine diorites of Subzone D, Luipershoek 140 JS.
9. Sulphides in olivine-bearing dioritic rocks of Subzone D, below Magnetitite Seam 21. Bore-hole DDH2, Doornpoort 171 JS.
10. Mineralized anorthosite below Magnetitite Seam 21, Duikerskrans 173 JS (Liebenberg, 1970, p. 193).
11. Mineralized anorthositic rock, 20m below Magnetitite Seam 21. Bore-hole DDH2, Doornpoort 171 JS.
12. Sulphides in the Magnetitite Seam 21. Bore-hole DDH2, Doornpoort 171 JS.
13. Sulphides in olivine-bearing diorites above Magnetitite Seam 21, Bore-hole DDH2, Doornpoort 171 JS.
14. Sulphides in the uppermost dioritic rocks from Tauteshoogte.

and chemical formulae as given in Dana (Ford, 1955). These results are presented diagrammatically in Fig. 54B. The distribution of the elements in the sulphide phase shows smooth variations with height in the intrusion. There is a very gradual increase in the sulphur content from 38, 2 per cent at the base of the Upper Zone to 39, 6 per cent in the olivine diorite above Magnetitite Seam 21. Above

FIG. 54A. VARIATION OF MINERALS IN THE SULPHIDE PHASE OF THE UPPER ZONE

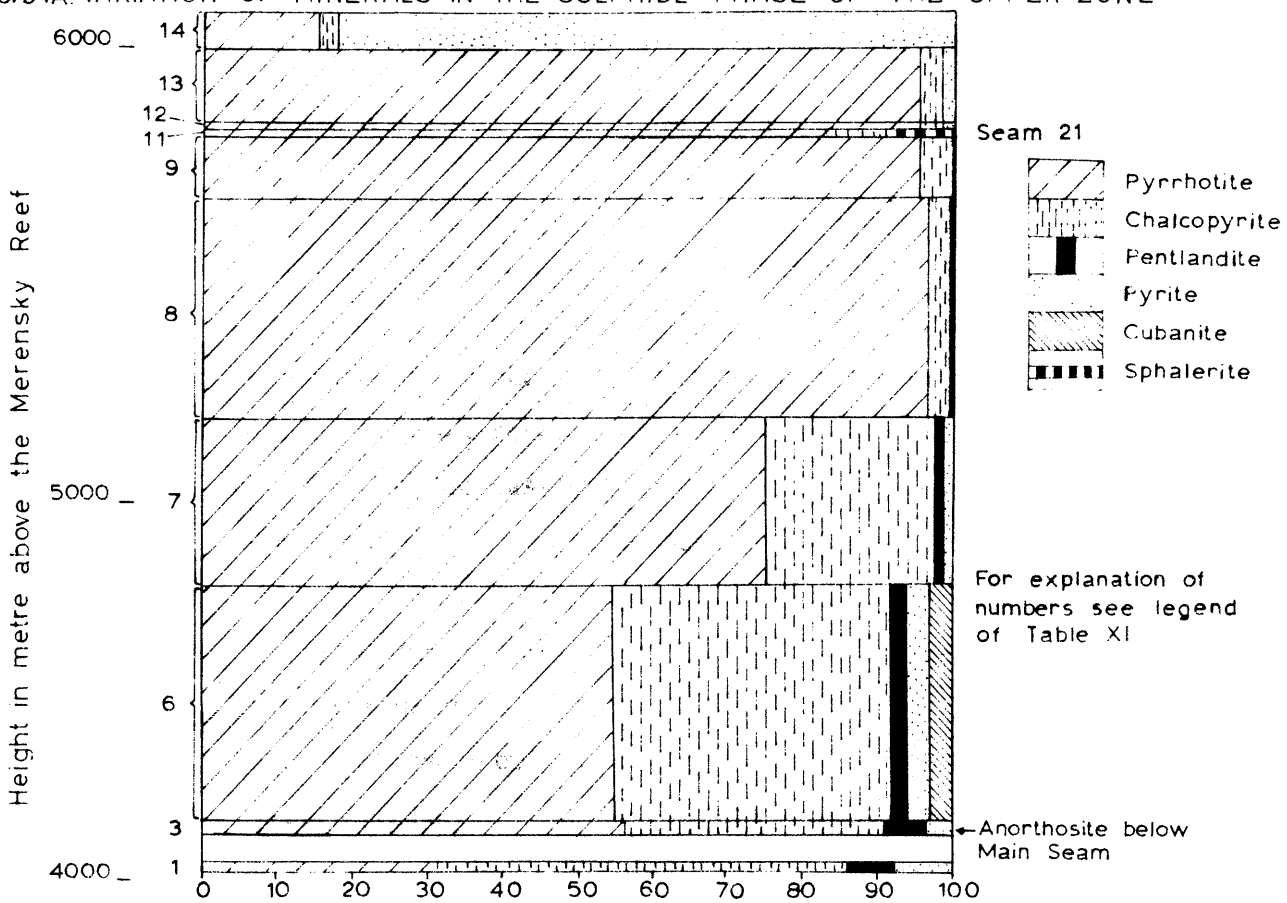

FIG. 54B. VARIATION OF ELEMENTS IN THE SULPHIDE PHASE OF THE UPPER ZONE

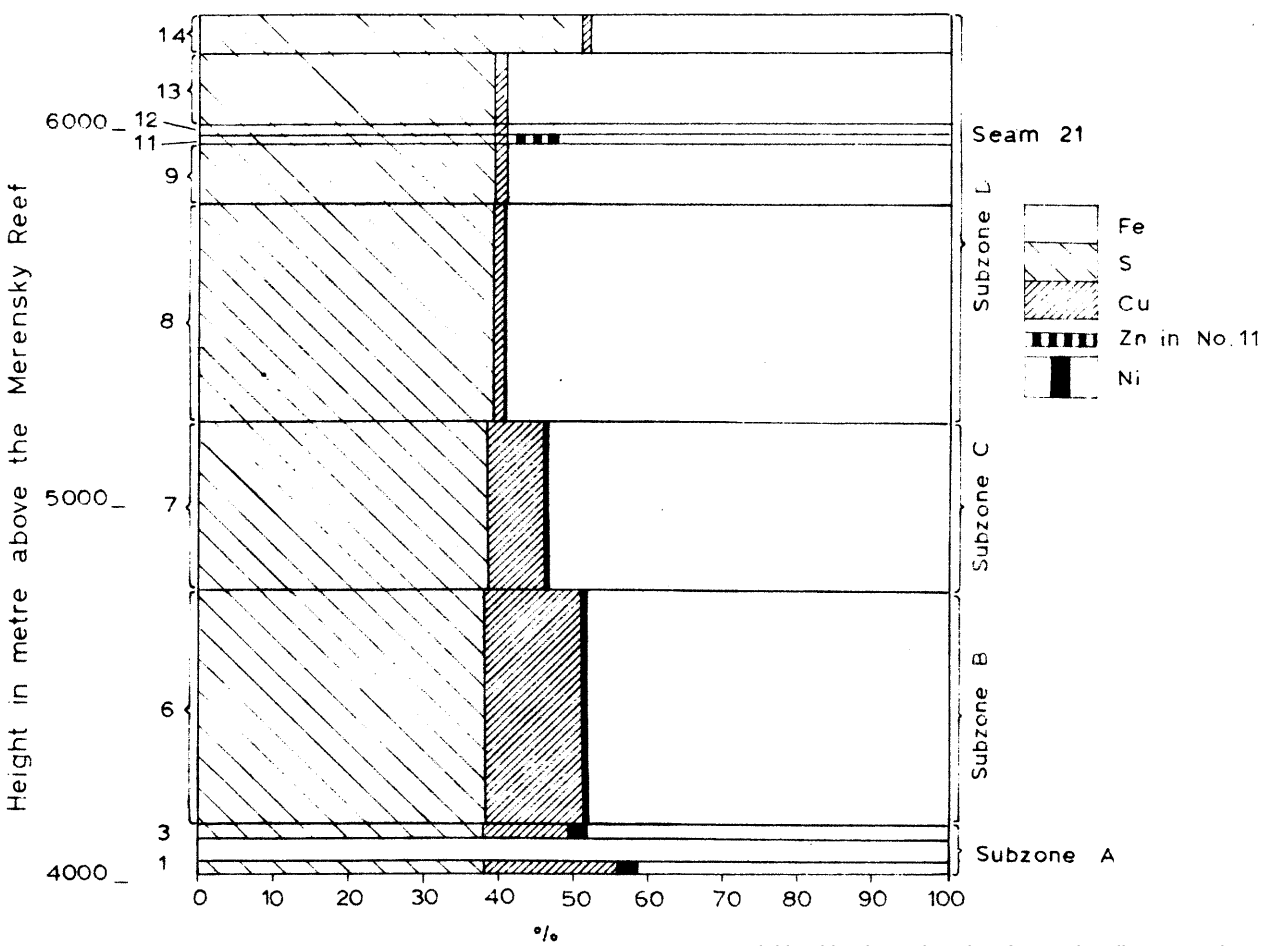

this horizon there is a sharp increase to 51 per cent in the topmost differentiates of the intrusion.

The behaviour of Cu and Ni with height is analogous to that of chalcopyrite and pentlandite (Figs. 54A and B) respectively. The Fe content increases fairly rapidly in the lower half of the Upper Zone, remains fairly constant at its maximum of about 59 per cent in the olivine-bearing rocks in the upper half of the Upper Zone, and drops sharply to 48 per cent at the top of the intrusion.

These modal analyses therefore show:

a) A decrease of chalcopyrite and pentlandite in the normal magnetite (olivine-free) gabbroic rocks in the lower half of the Upper Zone together with a concomitant increase in the pyrrhotite content.

b) A relatively constant pyrrhotite-chalcopyrite ratio in the olivine-bearing dioritic rocks in the upper half of the Upper Zone.

c) An abrupt increase of pyrite and a decrease of pyrrhotite in the top 100m of the intrusion.

Before the significance of these trends is discussed any further with the aid of published phase diagrams, it is necessary to describe briefly the textures of the sulphide minerals in the various horizons.

3. Description and textural features of the sulphides

a) The sulphides in the anorthosite below Lower Seam 2 (1, Table X)

Underlying the Lower Magnetitite Seam 2 is a mottled anorthosite, 1,5m thick, which contains disseminated sulphides at its top. In the riverbed on the farm, Zwartkop, 142 JS, 0,5km to the north of the area investigated, there is a concentration of sulphides at this horizon, with the result that sulphides are present throughout the anorthosite, a few specks also being found in the underlying magnetite gabbro. This enrichment in sulphides was observed for about 10m along strike on both sides of the riverbed.

Five polished sections of this occurrence were examined and the sulphides identified are chalcopyrite, pyrrhotite, pentlandite and pyrite, as well as the alteration products of pyrrhotite and pentlandite, namely, melnikowite-pyrite and bravoite, respectively. In addition to these, a small amount of sphalerite was found in association with the chalcopyrite. The chalcopyrite also contains a few very small specks of blueish-white, probably platinum-bearing, minerals.

Point count analyses were carried out on four of the polished sections and the result is given in Table XII. According to this modal analysis, the anortho-

TABLE XII POINT COUNT ANALYSIS OF THE MINERALIZED ANORTHOSITE BELOW LOWER MAGNETITITE SEAM 2

Mineral	Points counted	Vol. %	Wt. %
Chalcopyrite	2636	1, 96	3, 00
Pyrrhotite	1488	1, 11	1, 86
Pentlandite	275	0, 21	0, 37
Pyrite	380	0, 28	0, 50
Ilmenite	95	0, 07	0, 12
Silicates (more than 99% plag.)	129 441	96, 37	94, 15
	134 315	100, 00	100, 00

Total area counted: 21, 2 sq. cm.

site contains 1, 04% Cu, 0, 12% Ni and 2, 9% S. This may therefore be considered as a comparatively rich mineralized horizon, and consequently two samples were sent for chemical analyses to the Anglo American Corporation of S. A. Ltd., the owners of the mineral rights. Their results are listed in Table XIII.

TABLE XIII PARTIAL CHEMICAL ANALYSES OF THE MINERALIZED ANORTHOSITE BELOW LOWER MAGNETITITE SEAM 2

Element	G562B	$G562B_1$	Average	Reported in
Copper	1, 10	0, 92	1, 01	per cent
Nickel	0, 18	0, 17	0, 175	"
Cobalt	0, 02	0, 02	0, 02	"
Zinc	0, 01	0, 01	0, 01	"
Arsenic	0, 005	0, 002	0, 004	"
Sulphur	2, 23	2, 30	2, 27	"
Platinum	0, 76	0, 83	0, 80	g/ton
Palladium	0, 76	0, 96	0, 86	"
Gold	0, 40	0, 47	0, 44	"
Silver	1, 52	1, 46	1, 49	"
Total precious metals	3, 44	3, 72	3, 59	"

The sulphides, magnetite and ilmenite are intercumulus and from textural relationships it seems as if the sulphides were the last to crystallize because they are moulded around the relic titanomagnetite grains.

Chalcopyrite is the main sulphide mineral. It is present as large grains which contain small blebs of pyrrhotite, and also as lens-like or lamellar exsolution-bodies in pyrrhotite. Sphalerite, in small patches, is intimately associated with the chalcopyrite. In one chalcopyrite grain a small asterisk-like exsolution of sphalerite was observed.

Apart from exsolution blebs and lamellae of chalcopyrite, pyrrhotite also contains flames and lamellae of pentlandite, both exsolved parallel to the (0001) direction. The hexagonal variety of pyrrhotite is the most common and contains only a few lamellae of the low temperature monoclinic variety. The pyrrhotite of this horizon is altered in places to a dull, light grey, lamellar, isotropic mineral, probably melnikowite-pyrite (Liebenberg, 1970, p. 140). Where this mineral is present, alteration was complete and rims around unaltered pyrrhotite were never observed. A certain amount of resorption of pyrrhotite has taken place after exsolution of the pentlandite lamellae and can be seen from pentlandite lamellae which protrude for a small distance into the surrounding silicates. In extreme cases, all the pyrrhotite around such lamellae was resorbed with the result that only pentlandite lamellae which have the same orientation as those in the nearby pyrrhotite remain (Fig. 55).

Pentlandite has a twofold mode of occurrence in this ore, namely, as exsolution-lamellae and flames concentrated along grain boundaries in the pyrrhotite and occasionally in the chalcopyrite (Fig. 56), as well as discrete grains at the margin of larger pyrrhotite grains. Where chalcopyrite is present, the pentlandite is always developed between the chalcopyrite and the pyrrhotite. The granular pentlandite exhibits an octahedral cleavage and fracturing, which is due to its high coefficient of thermal expansion (Morimoto and Kullerud, 1964, p. 205). Pentlandite alters to bravoite which is slightly more red and has a lower reflectivity. Rims of alteration are often found around unaltered pentlandite. Bravoite may be present together with unaltered pyrrhotite but where pyrrhotite has altered to melnikowite-pyrite, all the pentlandite is altered to bravoite.

Pyrite is present as rims around all the other sulphides. It is usually separated from them by a thin rim of late silicates and in most cases is seen to

replace early formed silicates. This seems to indicate that pyrite was the last sulphide to crystallize.

No magnetite was observed in any of the sections investigated, although skeletal ilmenite, typical of the exsolution texture in magnetite, indicates that it was present at an early stage. In many sections from the Upper Zone, the pyrrhotite has either replaced magnetite or filled cavities left by the dissolution of the magnetite (Fig. 57). The exsolved ulvospinel is oxidised to ilmenite, although the delicate exsolution texture is in most cases preserved.

b) Sulphides in the magnetite gabbros of Subzone A

Three polished sections of magnetite gabbros from Subzone A were investigated. The sulphide content in all the sections is very low. From visual estimates, chalcopyrite and pyrrhotite are the most common sulphides and are present in approximately equal amounts. The other sulphides are pentlandite and pyrite.

c) The sulphides in the anorthosite below the Main Magnetitite Seam (3, Table X)

The sulphides in this anorthosite have been described by Liebenberg (1970, p. 193). One of his samples comes from the Roossenekal area, and it is not necessary to repeat the textural relations. One sample (G655) of this anorthosite was collected by the author in Zwartkop 142 JS and point counts on two polished sections were made (Table XIV).

TABLE XIV MODAL ANALYSIS OF THE MINERALIZED ANORTHOSITE (G655) BELOW THE MAIN MAGNETITITE SEAM. ZWARTKOP 142 JS

Mineral	Points counted	Vol. %	Wt. %
Chalcopyrite	767	1, 3	1, 97
Pyrrhotite	1196	2, 0	3, 37
Pentlandite	117	0, 2	0, 35
Pyrite	71	0, 1	0, 21
Ilmenite	4		
Plagioclase	57 353	96, 4	94, 1
	59 508	100, 0	100, 00

Total area counted: ± 10, 0 sq. cm.

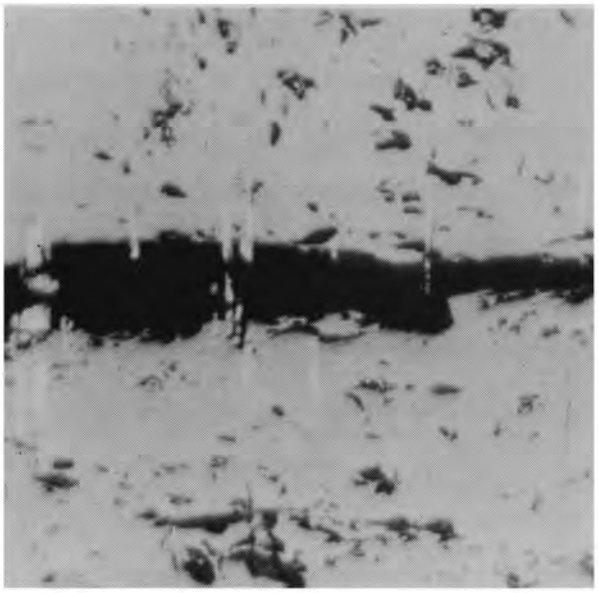

Fig. 55. Exsolution-lamellae of pentlandite protruding into gangue due to replacement of pyrrhotite. Mineralized anorthosite below Lower Seam 2 (G562B). Reflected light, x250.

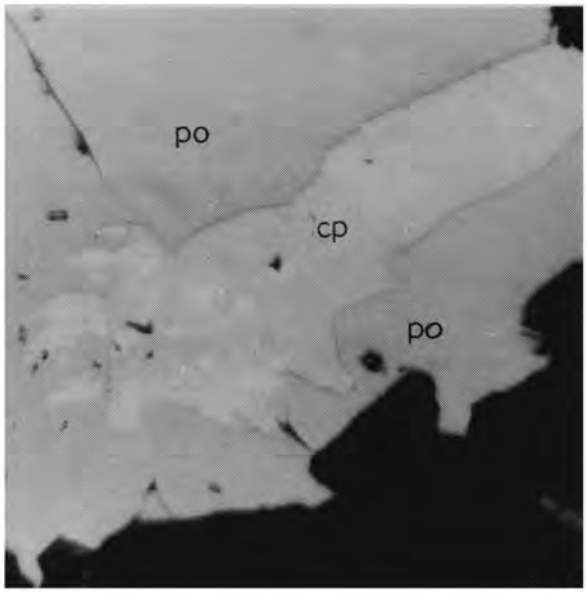

Fig. 56. Pyrrhotite containing exsolved chalcopyrite and pentlandite. Pentlandite (white) is present as exsolution flames in pyrrhotite (po) as well as in chalcopyrite (cp). Mineralized anorthosite below Lower Seam 2 (G562B). Reflected light, x250.

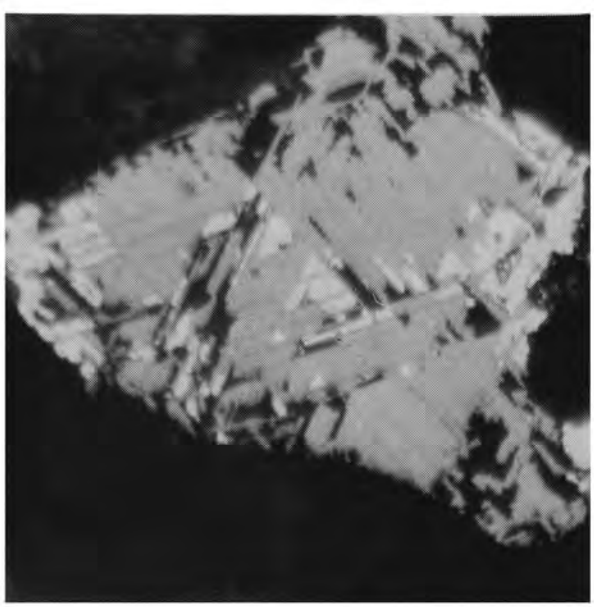

Fig. 57. Pyrrhotite and gangue replacing magnetite but not ilmenite. Olivine diorite (DDH2-229) Reflected light, x250.

According to this volumetric analysis the anorthosite at this locality contains 0,68% Cu, 0,11% Ni and 2,26% S.

The textures of the sulphide minerals are essentially the same as those described in the previous section. The only differences are that the pyrite does not form late rims around the other sulphides, but is present as grains within pyrrhotite. In these sections it can clearly be seen that alteration of pyrrhotite to melnikowite-pyrite starts along the grain boundaries and cracks in the pyrrhotite and advances more rapidly parallel to the (0001) plane of the pyrrhotite.

When the volumetric composition of the sulphides is compared with similar analyses cited by Liebenberg (Table X, Nos 2, 3 and 4) then it is striking how little the composition varies from one locality to the next. Only the pyrrhotite and pyrite content varies which may be explained by small differences in the S content of the sulphide phase.

d) The sulphides in the magnetite gabbros of Subzone B (6, Table X).

The sulphide phase of this horizon is characterized by the presence of cubanite, which occurs as lamellae and blebs in pyrrhotite as well as in chalcopyrite, and is readily distinguishable from chalcopyrite by its paler yellow colour and more lively anisotropism. In one section (G652) thin lamellae of pentlandite were observed in the cubanite. The textures of the other sulphide minerals are similar to those described in the previous chapters.

In certain sections, (G510, G569) pyrrhotite and pentlandite are partially altered to melnikowite-pyrite and bravoite. Wherever these alteration products were encountered in the sequence, they were regarded as the original product. The final alteration product of melnikowite-pyrite seems to be pyrite, but it is often difficult to discern whether the latter has not replaced pyrrhotite at a later stage. The pyrite in the two sections G510 and G569 is however only present where pyrrhotite has been altered to melnikowite-pyrite, and the impression gained is that the pyrite is not part of the primary sulphide minerals.

e) The sulphides in the magnetite gabbros of Subzone C (7, Table X).

The sections investigated of the olvine-bearing rocks of the Sisal Horizon contained very little sulphides and a point count analysis of the few specks encountered would not have been very reliable. Liebenberg (1970, p. 142, Fig. 25) gives an estimate of the composition of the sulphide phase of this horizon and records the absence of chalcopyrite. Sections investigated in this study, however,

showed that chalcopyrite and pyrrhotite are the most abundant sulphides in this horizon. The olivine-bearing rocks from the Sisal Horizon are relatively thin and would not greatly affect the trends observed in the larger rock units.

The sulphide phase in the overlying magnetite gabbro is enriched in pyrrhotite compared to the underlying magnetite gabbros, and also contains considerably less chalcopyrite. Cubanite is absent in these rocks and a small amount of pyrite was observed in one of the four sections investigated. This pyrite is not associated with the other sulphide minerals, but is present as irregular isolated patches and therefore does not seem to be part of the primary sulphide phase.

The textural relationships are similar to those described from lower horizons.

f) The sulphides in the olivine diorites of Subzone D (8, Table X)

A few interesting changes occur at the base of this subzone. The first of these is a sudden increase in the pyrrhotite content from about 75 per cent in the underlying olivine-free gabbroic rocks to more than 95 per cent. This high pyrrhotite content is characteristic of all the olivine-bearing rocks in the upper half of the Upper Zone. The second change, which was already noticed in a section (G642) high up in the previous rock unit, but which is present throughout the olivine-bearing rocks higher up, is that the sulphides occur in small rounded to elongated droplets on an average 0,25 x 0,15mm in size, fairly evenly distributed throughout the rocks. In rocks from lower horizons, the sulphides are essentially interstitial and have very irregular outlines. A further characteristic is that many of the small rounded droplets are either enclosed in or developed at the margins of the titanomagnetite and ilmenite grains. This would seem to indicate that the sulphides crystallized before or simultaneously with the oxide minerals, whereas in lower horizons of the Upper Zone, the sulphides crystallized after the oxide minerals. Another change noticed was that the olivine-bearing rocks in the upper half of the Upper Zone contain a fairly uniform content of 0,5 per cent sulphides, compared to the rather erratic and usually much lower values of the olivine-free gabbros of the lower half of the Upper Zone.

The textural relations of the minerals in the sulphide phase remain essentially the same. The low Ni and Cu content (8, Table XI) of the sulphide phase results in the absence of pentlandite and chalcopyrite as discrete grains. These

two minerals occur as exsolution-lamellae parallel to the basal plane of the pyrrhotite. Small blebs of chalcopyrite are occasionally found to be developed at the margin of the pyrrhotite grains but are also considered to have originated by exsolution of chalcopyrite from pyrrhotite.

A small amount of cubanite and mackinawite was noticed in one section (G634). The latter is present as thin exsolution-lamellae in pyrrhotite and was identified by its strong pleochroism from dark grey to white, and its characteristic black and white anisotropism under crossed nicols.

g) Sulphides in olivine-bearing diorites between Magnetitite Seams 17 and 21

The rock types developed between Seams 17 and 21 either contain very little olivine or are olivine-free. It was also noted (see chapter on lateral variation of facies) that the amount of olivine in this part of the sequence increases gradually in a southerly direction, and also in a westerly direction as indicated by the olivine-bearing rocks intersected below the 21st Seam in bore-hole DDH2 on the farm Doornpoort 171 JS. The sulphides described from this portion of the sequence were studied from material obtained from this bore-hole. Sections of samples from olivine-free rocks in this part of the sequence contain very little sulphides. It must be mentioned that of the six samples investigated, three were taken from above the mineralized anorthosite described in the next section, and that three were taken from below that horizon.

The presence of what may be described as secondary sulphides, is characteristic of the olivine-bearing rocks in this and higher horizons. These secondary sulphides were already noted in small quantities at the top of the previous rock unit, but they contribute quantitatively much more to the modal composition in the higher horizons. They can be distinguished fairly readily from the primary types in that the former do not occur as droplets and in that they are associated with late stage alteration products of olivine and magnetite.

Pyrrhotite is the most common of these secondary sulphides, although some pyrite was observed together with the pyrrhotite in the uppermost magnetitite seam. Where this pyrrhotite occurs together with altered olivine, secondary magnetite, serpentine or ilvaite are invariably present.

A texture that is fairly common in these rocks is magnetite which is dissolved, leaving behind a skeletal texture of exsolved ilmenite. These resorbed areas are usually filled with chloritic material but in some places also by pyrrhotite (Fig. 57) which must necessarily be of a later generation than the

pyrrhotite of the droplets. All the secondary pyrrhotite is of the low temperature monoclinic variety.

h) The mineralized anorthosite 20m below the Uppermost Magnetitite Seam (11, Table X)

Strictly speaking, this is not a pure anorthosite as are those developed below lower magnetite seams, but contains fair amounts of hornblende and biotite. It is some 3m thick and is in places anorthositic. Olivine is conspicuously absent and the rock is considerably coarser grained than the over- and underlying olivine-bearing gabbros. Granophyrically intergrown quartz and K-feldspar is present in places.

The composition of the sulphide phase differs considerably from that of the over- and underlying olivine-bearing rocks (Table X). Although pyrrhotite is by far the most abundant sulphide, it is practically devoid of pentlandite.

Sphalerite is a common constituent of this rock type and comprises about 35 per cent of the sulphides in one section (DDH243). It is intimately associated with chalcopyrite and usually occurs as grains at the margin of, and as small blebs in, chalcopyrite. Exsolved in the sphalerite are numerous small round blebs of chalcopyrite (Fig. 58). Small amounts of galena are associated with the sphalerite. The sulphides are present as roundish blebs, usually about 3mm in diameter, but occasional larger concentrations of up to 1cm in diameter are developed.

The composition of the sulphide phase at this locality differs considerably from that of the correlated mineralized anorthosite described by Liebenberg (1970, p. 193) from Duikerskrans 173 JS (Table X, Nos. 10 and 11). No reasonable explanation for this anomaly can be given, but the possibility cannot be excluded that owing to the change in rock sequence as already explained above, the anorthosite described by Liebenberg is not developed on Doornpoort 171 JS. The coarse-grained nature of the rock under discussion and the presence of hornblende, biotite, quartz and K-feldspar seems to indicate that this rock is a pegmatoid which would explain to some extent the differences in the composition of the sulphide phases recorded in Table X.

i) Sulphides in the Magnetitite Seam 21 (Table X, No. 12)

Fairly large amounts of sulphides are present in the Magnetitite Seam 21 where it was intersected in bore-hole DDH2 on the farm Doornpoort 171 JS. Apart from the numerous small drop-like sulphide concentrations in titanomagnetite grains (Fig. 59) or at the boundaries thereof, larger lens-like concentra-

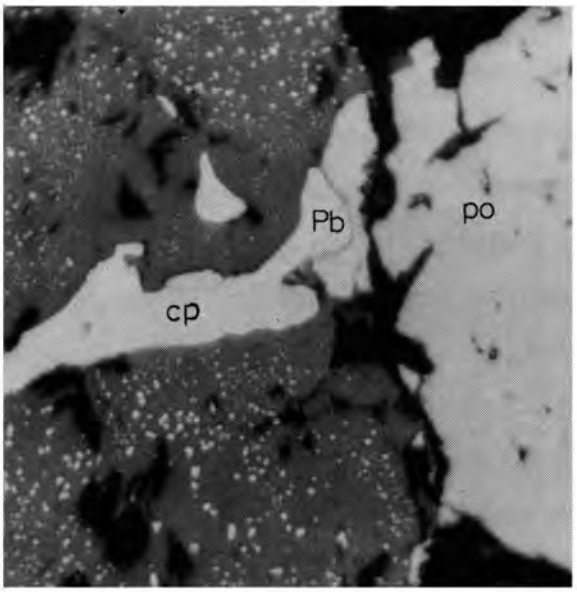

Fig. 58. Sphalerite (dark grey, left) with numerous small exsolved blebs of chalcopyrite, chalcopyrite (cp), pyrrhotite (po) and galena (Pb) in mineralized anorthositic pegmatoidal rock below Seam 21. (DDH2-243). Reflected light, x250.

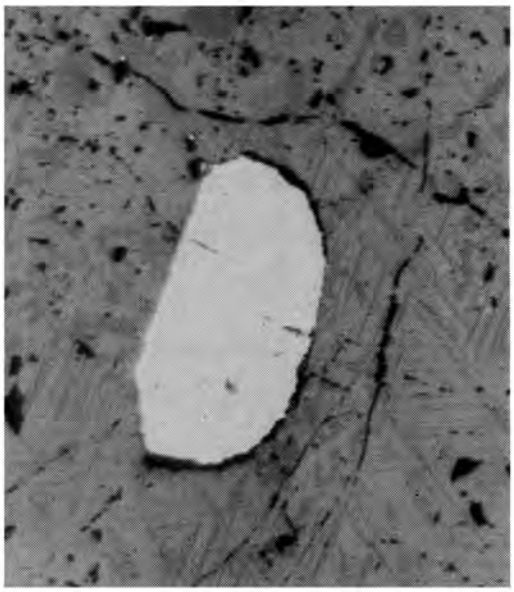

Fig. 59. Typical sulphide droplet (pyrrhotite) in titanomagnetite. Seam 21, (DDH2-160). Reflected light, x250.

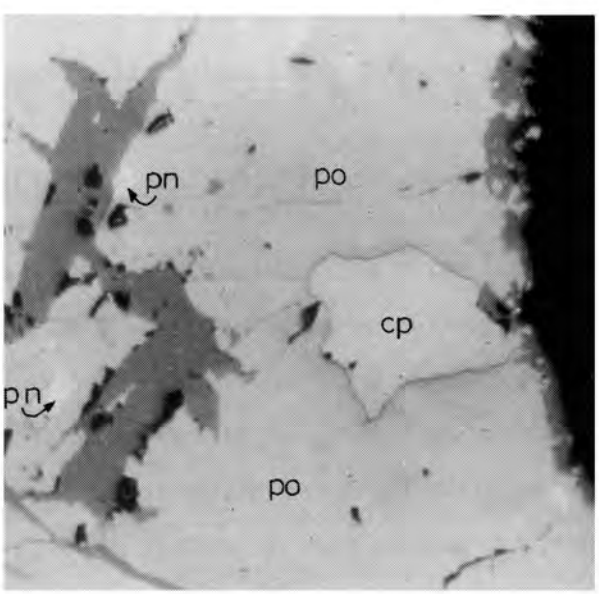

Fig. 60. Magnetite (grey) at the margin of and as stringers in the sulphide phase. Pyrrhotite (po), pentlandite (pn) and chalcopyrite (cp). Seam 21 (DDH2-162). Reflected light, x250.

tions of sulphides are present throughout the whole seam. These concentrations vary in size but are usually 1cm long and a few mm thick, and orientated parallel to the plane of layering.

The composition of the sulphide phase is essentially similar to that of the underlying olivine-bearing gabbro. Some of the pyrite present is associated with the pyrrhotite. Pure magnetite is present as stringers on the borders of, and as patches in, the larger sulphide grains (Fig. 60).

Secondary pyrrhotite is quite common and is associated with the altered olivine grains which are present throughout the seam.

j) Sulphides in the olivine diorites above Seam 21. (Table X, No. 13)

The composition and texture of the sulphides from this horizon are similar to those of the lower-lying olivine-bearing gabbroic rocks and need not be repeated here.

k) Sulphides in the uppermost differentiates (diorites) of the Bushveld Complex (Table X, No. 14)

There is a fairly rapid, but smooth change in the composition of the sulphide phase from the olivine-bearing diorite to the relatively olivine free diorite at the top of the intrusion. Pyrrhotite is still quite common in the lower portion of the diorite (G216, G207), but is very rare at the top of the intrusion where pyrite and chalcopyrite are the most common sulphides (G214, G215). Accompanied by this change is a fairly sharp drop in the sulphide content of the rocks.

4. Interpretation of the textural features and the observed mineral assemblages with the aid of phase diagrams

a) A brief description of the phase relations in the Cu-Ni-Fe-S System

Because many of the Ni-Cu ores of the world are associated with mafic and ultramafic rocks and because the major sulphide minerals in these rocks are essentially combinations of pyrrhotite, chalcopyrite, pentlandite and pyrite (as well as a number of other minor sulphides) much attention has in recent years been given to the Cu-Fe-Ni-S system. A vast amount of literature exists on various components of this system but the most significant recent article is that by Craig and Kullerud (1969, p. 344-358) who, apart from original investigations, have compiled the relevant published data, to give a detailed description of the phase relations in the Cu-Ni-Fe-S system. To interpret the textural and compositional variations in the sulphide phase of the Upper Zone, extensive use has been made of their article, which thus obviated the necessity of having to refer

to many other publications. However, before discussing the various textures observed, it is perhaps advisable to give a brief explanation of the more important reactions which occur in the Cu-Ni-Fe-S system. Only those reactions which involve phases observed are given.

At very high temperatures, well above 1000°C, the Cu-Ni-Fe-S system consists of Cu-Ni-Fe- alloys which coexist with sulphide liquid. This sulphide liquid is separated from the sulphur liquid by a large field of liquid immiscibility (Craig and Kullerud 1969, p. 347). The first sulphide of interest to this study to crystallize is a pyrrhotite-rich Fe-Ni monosulphide solid solution (Mss). This Mss appears as $Fe_{1-x}S$ on the Fe-S join at 1129°C and on cooling rapidly extends across the Fe-Ni-S face and joins $Ni_{1-x}S$ at 992°C to form a region of complete solid solution between $Fe_{1-x}S$ and $Ni_{1-x}S$ (the so-called Mss) (ibid., p. 348). At 743°C the iron-rich portion of the Mss reacts with sulphur liquid to form pyrite and tie lines exist between pyrite and the Fe-rich portion of the Mss. At 826°C the phase $Ni_{3\pm x}S_2$ appears at the Ni-S boundary of the Fe-Ni-S system and tie lines exist between $Ni_{3\pm x}S_2$ and the Mss. The $Ni_{3\pm x}S_2$ phase reacts at 610°C with the Mss to form pentlandite and tie lines between this new phase and Mss are established.

Below 600°C the width of the Mss field in the Fe-Ni-S system decreases gradually as a result of the formation of more pyrite in the more sulphur-rich part of the Mss and the exsolution of Ni as pentlandite in the more metal-rich portion of the Mss. Only below temperatures of 300°C is solid solution between $Fe_{1-x}S$ and $Ni_{1-x}S$ no longer complete and can tie lines between pentlandite and pyrite be established. (Craig and Kullerud, 1969, p. 350-352).

Above 320°C, the pyrrhotite ($Fe_{1-x}S$) of the Mss is of the high temperature hexagonal variety. Below this temperature it inverts to a low temperature hexagonal variety which, in the presence of pyrite, inverts to a monoclinic variety below 310°C (Kullerud 1967, p. 290-291).

The pentlandite which exsolves from pyrrhotite below 610°C has a lower sulphur : metal ratio than the pyrrhotite, with the result that the pyrrhotite is enriched in sulphur. This excess in sulphur will also cause the inversion of some of the hexagonal pyrrhotite to low temperature monoclinic pyrrhotite below 310°C.

From the above it is obvious that at low temperatures, pyrite can coexist with monoclinic pyrrhotite, but not with hexagonal pyrrhotite. Pyrite may however be found in the presence of hexagonal pyrrhotite. This is ascribed by

Naldrett and Kullerud (1967, p. 502) to the stable character of pyrite, which, once formed, does not react rapidly with hexagonal pyrrhotite to form monoclinic pyrrhotite.

The pyrrhotite of the Mss can take approximately 2 wt. per cent Cu into solid solution at high temperatures (Yund and Kullerud, 1966, p. 466) and exsolves as chalcopyrite from the pyrrhotite at temperatures below 450°C (Craig, 1966, p. 335).

A field of chalcopyrite solid solution appears in the Cu-Fe-S system at 970°C (Craig and Kullerud, 1969, p. 348). The chalcopyrite solid solution breaks up at 590°C into two phases, namely chalcopyrite and cubanite. At this temperature tie lines exist between cubanite and pyrite and therefore prevent the coexistence of chalcopyrite and pyrrhotite. At 334°C however, cubanite and pyrite react to form chalcopyrite and pyrrhotite (Yund and Kullerud, 1966, p. 485). Tie lines are again established between pyrrhotite and chalcopyrite below 334°C with the result that the association of cubanite and pyrite is unstable below this temperature.

From the above description of the phase changes on cooling of a sulphide phase with a composition that falls within the Cu-Fe-Ni-S system, it is obvious that the three most common mineral assemblages are (Craig and Kullerud, 1969, p. 352):

i) Chalcopyrite + pyrite + monoclinic pyrrhotite + pentlandite.

ii) Chalcopyrite + monoclinic pyrrhotite + hexagonal pyrrhotite + pentlandite.

iii) Chalcopyrite + cubanite + hexagonal pyrrhotite + pentlandite.

b) Discussion of the mineragraphy in the light of the phase relations in the Cu-Ni-Fe-S system

It is generally believed (Craig and Kullerud, 1969, p. 355) that at high temperatures, liquid immiscibility exists between sulphide liquid and gabbroic melt. Magnetite-pyrrhotite assemblages begin to melt at 1050°C if the pyrrhotite contains 60,5 weight per cent Fe. A rise in the iron content of the pyrrhotite to 62,8 weight per cent Fe has the effect of lowering the melting temperature to a minimum of 934°C (Naldrett, 1969, p. 177 and Fig. 6). The substitution of 2 weight per cent Cu for iron in the pyrrhotite lowers the melting temperature by 15-20°C, whereas the presence of Ni has apparently no effect (ibid., p. 180).

Although no magnetite was observed in the sulphide phase, except in that

from the Magnetitite Seam 21, the nature of the ore is such, that diffusion of oxygen from the separated sulphide liquid to the surrounding magma could have taken place, to prevent the crystallization of magnetite (Naldrett, 1969, p. 192; see below). It therefore seems unlikely that crystallization of the pyrrhotite commenced at temperatures above 1050°C. Where the sulphide phase is interstitial to the silicates, as is the case for the lower half of the Upper Zone, the crystallization temperature of the silicates must have been considerably higher than that of the sulphides. Chalcopyrite is present in large quantities in this ore and apart from the 4-5 per cent of this mineral which has exsolved from pyrrhotite below 450°C, the bulk of the chalcopyrite seems to have crystallized from the residual Cu-rich sulphide liquid at approximately 970°C.

On the grounds of the texture and estimated composition of crystalline sulphide droplets in lava from Hawaii, Skinner and Peck (1969, p. 319) concluded that the sulphide in these droplets crystallized above 1065°C as a Cu and Ni-rich pyrrhotite solid solution which contained as much as 9 weight per cent Cu. Although this does not agree with the experimental studies in the Cu-Fe-S system (Kullerud, 1968, p. 405) the presence of a Cu-rich pyrrhotite ss at high temperatures cannot be disregarded. The sulphide phase in the lower part of the Upper Zone contains more than 11 weight per cent Cu (Table XI) and the texture of the ore does not indicate that the bulk of the chalcopyrite has exsolved from a Cu-rich pyrrhotite ss.

The absence of pyrite associated with pyrrhotite in the mineralized anorthosite below Lower Magnetitite Seam 2 indicates that the sulphide phase was metal-rich. Seeing that these ores contain considerably less than 10 per cent Ni, all the pentlandite (i. e. discrete grains as well as exsolution-lamellae) has probably originated due to exsolution from the monosulfide solid solution at temperatures below 600°C (Naldrett and Kullerud, 1966, p. 322). The presence of pyrite in this anorthosite can be explained by an enrichment in sulphur in the last intercumulus silicate liquids which did not separate from the magma as part of the sulphide phase.

In contrast, the sulphide phase of the mineralized anorthosite below the Main Magnetitite Seam was richer in sulphur than the sulphide phase below the Lower Magnetitite Seam 2. This is seen by the presence of pyrite associated with pyrrhotite and indicates that reaction between pyrrhotite and sulphur took place below 743°C to produce pyrite. In this case, the composition of this ore lies on

the sulphur-rich side of the Mss with the result that all pentlandite probably formed below 300°C. This is similar to the sequence of events at the Strathcona Mine as described by Naldrett and Kullerud (1967, p. 504-505).

The sulphides in the magnetite gabbros of Subzone B are characterized by the presence of cubanite. This is indicative of sulphur deficient ore and the chalcopyrite ss which crystallized at 970°C was probably Fe-rich for cubanite to form at 570°C. The formation of pentlandite therefore resembles the formation of that described in the sulphides in the mineralized anorthosite below Lower Magnetitite Seam 2. As has been mentioned earlier, the pyrite observed in two of the six sections investigated, seems to be secondary, and could have crystallized from the intercumulus liquid owing to an enrichment in sulphur which did not separate as part of the sulphide liquid.

The phase relations in the sulphide phase of the magnetite gabbros of Subzone C are essentially the same as those in the mineralized anorthosite below Lower Magnetitite Seam 2. The only difference is in the lower chalcopyrite and higher pyrrhotite contents.

The sulphides in all the olivine-bearing rocks above the magnetite gabbros of Subzone C can be discussed together.

It was observed by Naldrett (1969, p. 181) that the crystallization temperature of pyrrhotite is not greatly affected by pressure, and it can therefore be assumed that the crystallization temperature of this mineral remained fairly constant throughout crystallization of the Upper Zone. As has been stated previously, one of the major changes observed where large amounts of olivine appear at the base of Subzone D is, that the sulphide changes from an essentially interstitial ore to small droplets, mostly associated with the titanomagnetite but also partially enclosed in other silicates except olivine. This seems to indicate that, owing to a gradual enrichment of S in the magma and owing to a gradual decrease in the crystallization temperature of the silicates, both of which are the direct result of fractional crystallization, the sulphide liquid separated at an early stage to form small globules distributed evenly throughout the crystallizing magma.

The composition of the sulphide phase in this part of the layered intrusion falls practically on the Fe-S boundary of the Cu-Ni-Fe-S system and all the chalcopyrite and pentlandite formed due to exsolution of Cu and Ni in solid solution in the pyrrhotite.

Very small amounts of cubanite are present in the lower olivine-bearing rocks, and some pyrite, which formed from reaction of pyrrhotite with sulphur liquid is present in Seam 21. This indicates that there was a gradual increase in the S content of the sulphide phase.

The sulphide content of the dioritic rocks above Magnetitite Seam 21 drops fairly rapidly, so that the topmost differentiates of the intrusion contain no primary sulphides. The pyrite in these rocks probably originated from magmatic sulphur that remained in solution in the silicate magma and which was concentrated in the residual deuteric fluids. This sulphur which remained in solution in the magma after separation of the sulphide liquid, is probably also responsible for all the secondary pyrite which was observed in the magnetite gabbros of the lower half of the Upper Zone, as well as for the pyrrhotite, and occasionally also pyrite, associated with the deuteric alteration of the olivine in the upper half of the Upper Zone. A similar origin for the pyrite in the felsitic norite of the Sudbury Irruptive was suggested by Naldrett and Kullerud (1967, p. 517).

It has been noted above that the sulphide phase of Magnetitite Seam 21 contains magnetite as small stringers and grains at the borders of the larger sulphide grains (Fig. 60). This magnetite is characterized by the absence of Ti-rich exsolution-bodies and has probably crystallized from the sulphide-rich phase. The presence or absence of magnetite in sulphides has been explained in detail by Naldrett (1969) and depends solely upon equilibrium of oxygen fugacity between sulphide liquid and surrounding silicate liquid. Naldrett has shown that, when oxygen is lost from the sulphide liquid by diffusion to the surrounding silicate melt, pyrrhotite alone will crystallize. On the other hand, if oxygen remains in the sulphide melt, crystallization of pyrrhotite will enrich the remaining sulphide liquid in oxygen, with the result that magnetite will also crystallize. This explains the presence of magnetite in massive sulphide deposits, where effects of diffusion of oxygen to the silicate magma were less, compared with the absence of magnetite in cases where sulphide droplets did not separate from the magma. In the latter instance Naldrett (1969, p. 192) argues that equilibration of oxygen fugacity between droplets and host takes place during crystallization of the pyrrhotite, and in this way may lose all of its oxygen to the surrounding silicate melt. This was probably the case with all the sulphides throughout the crystallization of the Upper Zone, except those in the uppermost magnetitite seam. The oxygen fugacity in the surrounding magma must have been relatively

high during crystallization of this massive magnetitite seam, (although owing to the stabilizing effect of TiO_2 on iron oxides, titanomagnetite crystallizes at a lower oxygen fugacity than that required to crystallize magnetite from a sulphide liquid (ibid., p. 194))and diffusion of oxygen from the residual ore liquid to the surrounding magma must have been very slow. The result was a sufficient enrichment of oxygen in the residual sulphide melt to crystallize pure magnetite from it.

5. Events leading to the crystallization of sulphides in the Upper Zone

Skinner and Peck (1969, p. 311) have shown that, in a tholeiitic basaltic magma from Hawaii with an average S content of 100ppm, the only environment in which the S content can be increased to saturation point is in the interstitial liquids. They found that at between 1060 and 1070^{o}C a sulphide-rich phase separates from the interstitial silicate liquid and that the S concentration in this liquid was 380 $\pm$ 20ppm; the concentration necessary to saturate the magma at that temperature.

Liebenberg (1970, p. 197) has shown that the average S content of the Bushveld magma was in the vicinity of 150ppm and that the average S content of the Main and Upper Zones is 50 and 350ppm respectively. The question that arises is why the sulphur concentration in the Main Zone is so much lower than the average S content of the Bushveld. The only reasonable explanation seems that the nature of the processes responsible for the crystallization of the cumulates never allowed large amounts of intercumulus liquid to become trapped, possibly owing to adcumulus growth and/or filter pressing of the intercumulus liquids into the overlying magma, which consequently became gradually enriched in sulphur. During crystallization of the lower part of the Upper Zone, the S content of the magma was still not high enough for the separation of immiscible sulphide droplets. Only under special conditions did the sulphur concentration rise to saturation point and these conditions were apparently only achieved where sufficiently large amounts of liquid were trapped in the intercumulus spaces. Crystallization of a batch of magma at the bottom of the chamber, to give rise to a cyclic unit would favour enrichment of S in the crystallizing bottom layer and might give rise to sulphides at the top of the cycle as envisaged by Liebenberg (1970, p. 196). He explains the presence of intercumulus sulphides below the magnetitite seams with the aid of the ternary phase diagram FeS - magnetite - gabbroic silicates. The magnetitite seam is considered by him to represent the

beginning of a cycle of crystallization, followed by crystallization of magnetite and silicates. At the ternary eutecticum sulphides, magnetite and gabbroic silicates would crystallize, conditions which would probably prevail in the intercumulus liquids at the end of a cycle. The next cycle would again commence with crystallization of magnetite, to form a seam directly overlying mineralized anorthosite. Absence of sulphides below a magnetitite seam is attributed by Liebenberg to the disturbance of the cycle before its termination (beheaded unit) by a new convection current.

Whatever the origin of the sulphide mineralization in the anorthosites below the Lower Seam 2 and the Main Magnetitite Seam, these sulphides are interstitial and it seems as if the S concentration of the magma during crystallization of these rocks was still fairly low, but apparently considerably higher than during crystallization of the greater part of the Main Zone. As crystallization proceeded, the magma became gradually enriched in S, until, at a level somewhere between Seam 14 and the olivine diorites of Subzone D, crystallization of some plagioclase and olivine was sufficient to saturate the magma in S with the result that numerous small sulphide droplets are found in the overlying rocks. The S concentration in the last 1000 metres of the Bushveld magma must therefore have been very close to saturation, which would correspond to between 350-400ppm.

6. Concluding remarks

Although the olivine-bearing, dioritic rocks of the Upper Zone contain, on the average, more sulphides than the ordinary gabbroic rocks lower down in the sequence, a concentration of sulphides in these rocks would not yield a deposit of economic interest owing to the unfavourable composition of the sulphide phase. Sulphide concentrations in the lower half of the Upper Zone are however of economic importance owing to the favourable composition of the sulphide phase, which, apart from appreciable amounts of chalcopyrite, also contains fair amounts of pentlandite.

More attention should therefore be given to the known sulphide concentrations in the lower part of the Upper Zone. The mineralized anorthosite underlying the Main Magnetitite Seam has been known for quite some time, but this investigation has revealed the existence of a mineralized anorthosite below the Lower Magnetitite Seam 2. The chemical analysis of this anorthosite (Table XIII) shows that concentrations of economic importance are to be found in this horizon.

Although, with our present knowledge, these concentrations seem to be sporadic, it must be borne in mind that outcrops of these mineralized horizons are scarce and restricted to a few river sections in the Eastern Transvaal.

F. POSTCUMULUS CHANGES

The various types of postcumulus changes which are restricted to a particular mineral, such as myrmekite, interpenetration and zoning of plagioclase, as well as the inversion from pigeonite to orthopyroxene, have already been described in the previous sections on the particular minerals. The changes discussed below are therefore those in which two or more minerals are involved, as well as changes in the cumulus pile as such.

1. Symplektite

Complex symplektitic textures characterize most of the rocks of the Upper Zone. Very little is known about these textures in gabbroic rocks and the extremely fine nature of the intergrowths, which closely resemble myrmekite, make identification of the involved phases difficult. Three different types of symplektite seem to be developed and are described separately below. The first two types are probably closely related in origin and occur as an intergrowth surrounding magnetite but seem to have developed at the expense of plagioclase, whereas the third type is an intergrowth of magnetite and pyroxene.

a) Symplektite in gabbroic rocks of Subzone B and C of the Upper Zone often displays a concentric zoning (Fig. 61) which, from magnetite outwards, consists of:

i) an inner zone of flaky biotite which surrounds the magnetite grain;

ii) a central zone of "needles" of biotite projecting radially into

iii) an outer zone of symplektite which advances convexly into the surrounding plagioclase.

Usually only two of these zones are developed, the central zone of biotite needles being mostly absent. It is extremely rare that only needles of biotite are developed (Fig. 62) although flaky biotite often surrounds magnetite grains without the symplektitic outer reaction zone. The white matrix of the biotite "needles" in Fig. 62 has a slightly higher refractive index than the twinned plagioclase and, although it does not exhibit twinning, is considered to be a more calcic plagioclase.

In detail the outer zone of the symplektite resembles myrmekite closely in that the vermicules are thin and orientated perpendicularly to the advancing

Fig. 61. Complex symplektite which consists of an inner zone (dark grey) of biotite, a central zone of "needles" of biotite in plagioclase and an outer zone of myrmekite-like intergrowth of pyroxene and plagioclase.G396. Crossed nicols, x70.

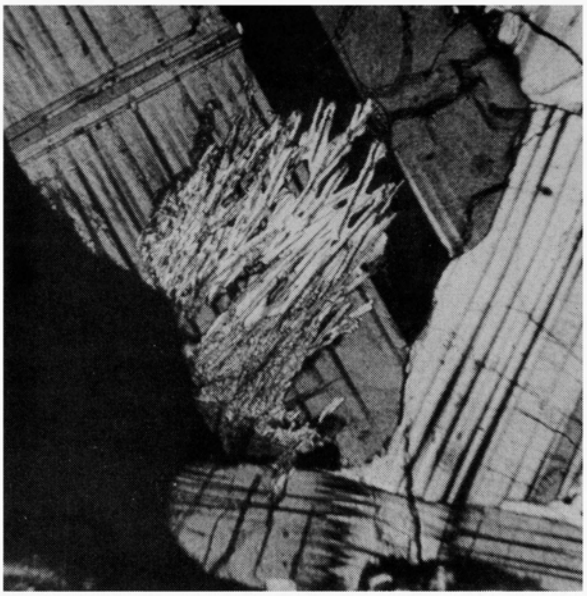

Fig. 62. Needles of biotite protruding into plagioclase. The white matrix between the "needles" is probably more calcic plagioclase. G396. Crossed nicols x70.

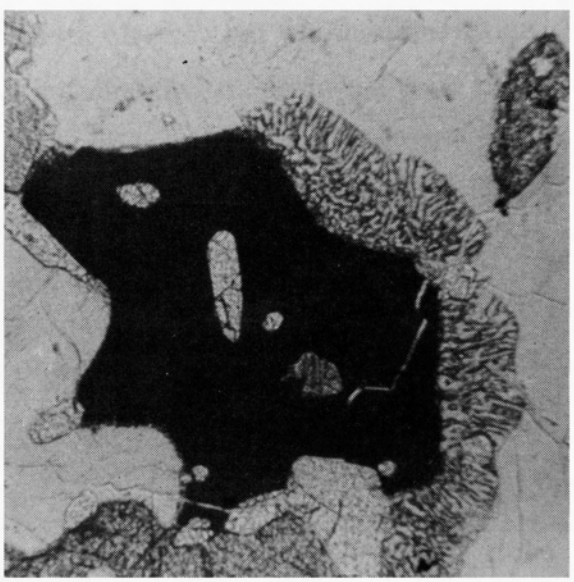

Fig. 63. Relatively coarse symplektite in olivine diorite The intergrowth probably consists of olivine and calcic plagioclase. G271. x70.

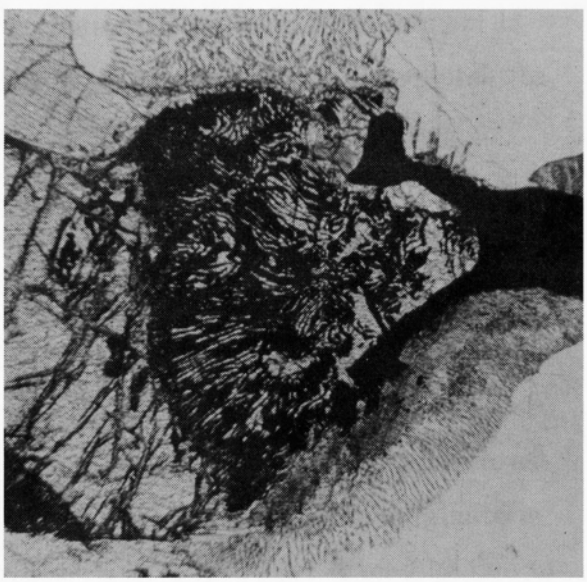

Fig 64 Symplektitic intergrowth of magnetite and pyroxene (centre). Olivine is to the left of the intergrowth. The more common type of symplektite at top and bottom. G621, x70.

"front" but coalesce towards the centre to form small irregular patches. The delicate texture makes it difficult to determine the mineral which constitutes the vermicules, but the higher relief and relatively low birefringence suggests that it may be orthopyroxene.

Symplektitic intergrowth of pyroxene and plagioclase was described by Molyneux (1964, p. 63 and p. 69) from the basal contact of the Main Magnetitite Seam and Seam 11.

b) The symplektite in olivine diorites of Subzone D of the Upper Zone differs from that of the olivine-free gabbroic rocks of the lower subzones in that biotite is scarce, so that the vermicular intergrowth is mostly the only zone present (Fig. 63). Where biotite is present it is always developed between the intergrowth and the magnetite. The intergrowth in these olivine-bearing rocks is slightly coarser than that of lower subzones and the vermicules have a considerably higher birefringence and refractive index than the plagioclase. Sometimes the mineral of these vermicules coalesces to form thin rims around the magnetite where it can be seen to consist of olivine.

c) A third type of symplektite, very seldom seen in thin section, consists of vermicular magnetite in pyroxene (Fig. 64). It is characteristically associated with olivine, but whether the olivine has contributed to the formation thereof is not certain. If, as is the case with myrmekite and the other types of symplektite, the intergrowth advances convexly outwards, then this type seems to have originated at the expense of olivine.

d) Origin of the symplektite

Various authors have described coronas around and reaction rims between certain types of minerals in gabbroic and anorthositic rocks (Buddington, 1939, p. 295-297 ; Huang and Merritt, 1954, p. 555; Murthy, 1958, p. 25-26) but they consider these textures to have originated by later metamorphism of these rocks. Buddington (1939, p. 295) mentions the possibility that coronas may originate by reaction of solid phases with deuteric intergranular fluid or that it may be due to discontinuous reaction between early formed crystals and residual (intercumulus) liquid. Herz (1951, p. 985 and p. 1015) considers that the symplektite in the Baltimore gabbro has originated in such a way. This hypothesis is also favoured by the author for similar intergrowths in the rocks of the Upper Zone.

The presence of either pyroxene or olivine, as well as biotite in these symplektite textures, which appear to be associated with more calcic plagioclase,

seems to suggest that a reaction between the last intercumulus liquid and the plagioclase has taken place. It is envisaged that an increase in the pH_2O would favour the formation of myrmekite, but instead of forming vermicules of quartz, these reacted with the intercumulus liquid to form ferromagnesian minerals, whereas any exsolved alkalis would react with this liquid to form biotite. As noted previously, myrmekite disappears in rocks where symplektite is developed, which may suggest that their origin is somehow related.

No satisfactory explanation can be offered at this stage for the magnetite-pyroxene symplektite.

2. Adcumulus growth and the intercumulus liquid

The initial porosity of the settled crystals in the accumulating mush is estimated as being between 20 and 50 per cent (Hess, 1960, p. 109; Jackson, 1961, p. 62; Wager and Brown, 1968, p. 60) with the result that the mechanism of enlargement of cumulus crystals to form adcumulates or monomineralic rocks with practically no pore material has puzzled many petrologists. As pointed out by Cameron (1969, p. 760) the preferred explanations are: firstly, that settled crystals continued to grow after shallow burial by diffusion of the required constituents into the crystal mush down a slight temperature gradient, a mechanism that was proposed by Hess (1961, p. 113), secondly, by enlargement while still in contact with the supernatant magma (Wager et al., 1960, p. 81 and Jackson, 1961, p. 62) and thirdly, by a combination of both processes mentioned.

As envisaged by Hess (1961, p. 113), the degree of enlargement of cumulus crystals by diffusion may be correlated with the rate of accumulation of crystals, i.e. where the rate of accumulation was slow, diffusion was operative, resulting in overgrowths of almost exactly the same composition as the cumulus crystals, and where accumulation was rapid, the original magma was effectively trapped.

Wager et al. (1960, p. 77) point out that for adcumulus growth, this process of diffusion "must have taken place at the same temperature as that of the formation of the cumulus crystals because of the similarity in the solid solution composition". They do, however, agree that enlargement of the cumulus crystals at constant composition did take place while they formed the uppermost layer of the pile and that thick layers of monomineralic rock must have formed very slowly. More recently, Wager (1963, p. 5 and Wager and Brown, 1968, p. 222)

suggests that adcumulus growth of settled crystals takes place on the top surface of a crystal pile. He argues that for crystal growth, heat has to be removed which, in ordinary circumstances, is lost into the surrounding lower temperature rocks. Conduction of heat from the top layer of accumulated crystals into the underlying crystal mush would not be sufficiently rapid for adcumulus growth to take place and he believes that the loss of heat must be into an overlying supercooled magma which is constantly brought in fresh supplies by convection into contact with the top surface of the cumulus crystals. Adcumulus growth can therefore continue as long as heat can be transferred into the overlying supercooled magma, providing that there is no fresh nucleation. This may be a reasonable explanation for adcumulus growth in the Skaergaard Intrusion where there is ample evidence for convection currents (Wager and Brown, 1968, p. 210-221).

Another mechanism whereby the amount of intercumulus liquid can be reduced, is compaction of the crystal mush prior to cementation, "if this were attended by re-solution of crystals at points of contact and redeposition in interstices" (Cameron, 1969, p. 759). Cameron however, states that owing to lack of evidence, this process has found little favour with students of magmatic sediments.

Compaction of the crystal mush is considered by the author to be one of the most important processes in the Bushveld Complex whereby large amounts of intercumulus liquid were pressed out of the pore spaces into the overlying magma. This is obvious from the various textural features displayed by the plagioclase crystals such as interpenetration, myrmekite, bent crystals and reversed zoning, the presence of all of which cannot, in the light of our present knowledge, be explained by another mechanism. An especially important mechanism whereby adcumulus growth can take place without having to assume large scale diffusion of the required constituents into, and the unwanted constituents out of, the pile of cumulus crystals, seems to be the process of re-solution, causing interpenetration and the redeposition of this material in the interstices. It is by no means suggested that compaction is the only process responsible for adcumulus growth, but that it may be just as important as diffusion after shallow burial or as enlargement of cumulus crystals while still in contact with the supernatant magma.